On the measurement and application of cement grout rheological properties

Tafadzwa John Shamu

Licentiate Thesis, 2019
KTH Royal Institute of Technology
School of Architecture and the Built Environment
Department of Civil and Architectural Engineering
Division of Soil and Rock Mechanics
Stockholm, Sweden

TRITA-ABE-DLT-1922
ISBN 978-91-7873-240-1

Akademisk uppsats som med tillstånd av KTH i Stockholm framlägges till offentlig granskning för avläggande av teknisk licentiatexamen onsdagen den 12 juni 2019 kl. 1300 i sal B26, KTH, Brinellvägen 23, Stockholm.

Abstract

The rheological properties of cement-based grouts play a key role in determining the final spread in grouted rock formations. Rheologically, cement grouts are known to be complex thixotropic fluids, but their steady flow behavior is often described by fitting the simple Bingham constitutive law to flow curve data. The resultant Bingham parameters are then used in grouting design of e.g. tunnels, to estimate the penetration length. Since cement grouts are thixotropic suspensions, the interpretation of their flow curves as obtained from flow sweeps in concentric cylinder rotational rheometers is often complicated by: the presence of wall slip, sedimentation and unstable flow at low shear rates. A systematic approach to study these effects within the constraints of the concentric cylinder geometry (Couette) and for different cement grout concentrations was carried out as part of the Licentiate research work. Of particular interest was the influence of geometry and flow sweep measurement interval on flow curves, including the characteristic unstable flow branch that appears at applied shear rates that are below the critical shear rate. The unstable flow branch observed below the critical shear rate has been described as a characteristic feature in the flow curves of thixotropic suspensions, e.g. cement grouts, laponite. From a practical standpoint, this information can then be readily used to improve rheological measurements of cement grouts. The existence of the critical shear rate below which no stable flow occurs, plus the complex wall slip phenomenon are then discussed by considering how they affect actual spread in rough and smooth rock fractures.

Another major part of the research presented in this thesis relates to the measurement of model yield stress fluid (YSF), i.e. Carbopol, velocity profiles within the radial flow geometry. Radial flow between parallel plates, is an idealized fundamental flow configuration that is often used as a basis for grout spread estimation in planar rock fractures. Compared to other flow configurations with YSFs, e.g. channels, only a limited amount of work has presented analytical solutions, numerical models and especially experimental work for radial flow. Thus, as a first step towards more systematic studies of the plug flow region of YSFs in radial flow the current work presents the design, manufacture and for the first time velocity profile measurements that were conducted by using the pulsed Ultrasound Velocity Profiling (UVP) technique. The current observations for tests carried out with different disk spacings and flow rates show a distinct plug region, coupled with wall slip effects for the Carbopol model YSF fluid that was used. The theoretically predicted velocity profiles and the measured ones agree reasonably well, and the main discrepancies are discussed. Future studies,

would then be targeted at improving the current experimental setup, for detailed measurements of the plug flow region along the radial length, which remains a challenging issue for studies on YSFs and engineering applications such as rock grouting design.

Keywords
Cement-based grouts, grouting, yield stress fluid (YSF), thixotropy, critical shear rate, radial flow, wall slip, Bingham model

Sammanfattning

Cementbaserade injekteringsmedels reologiska egenskaper har en stor påverkan på strömning och inträngningslängd i sprickigt berg. Medlens reologi är komplex, inklusive tixotropi, men strömningen beskrivs ändå oftast med den enkla linjära Bingham modellen i injekteringssammanhang. De två parametrarna från denna modell, flytgräns och viskositet, används sedan inom injekteringsdesign, för t.ex. tunnlar och dammar, för att bedöma inträngningen. Eftersom cementbaserade medel är tixoptropa suspensioner försvåras utvärderingen vid mätning med konventionella rotationsviskometrar på grund av glidning vid fasta begränsningsytor, sedimentation/separation av partiklarna och instabila flöden vid låga deformationshastigheter. En systematisk mätprocedur för att studera ovanstående problem med rotationsviskometer och koncentriska cylindrar samt olika vanliga vattencementtal, har utförts inom ramen för detta licentiatarbete. Av särskilt intresse har varit att studera effekten av olika geometrier och tidsintervallet mellan mätningarna, inklusive den instabila delen av flödeskurvan då deformationshastigheten är lägre än ett kritiskt värde. Denna del av kurvan har i litteraturen beskrivits som karakteristisk för tixotropa suspensioner, som t.ex. cementbaserade injekteringsmedel. Praktiskt kan ovanstående kunskap användas för att förbättra mätningen av de reologiska egenskaperna. Existensen av en kritisk deformationshastighet under vilken det inte finns något stabilt flöde, i kombination med glidning vid fasta begränsningsytor, diskuteras särskilt med hänsyn till dess påverkan på faktisk inträngning i släta och råa bergsprickor.
Ett annat fokus i licentiatarbetet har varit att studera icke-Newtonska modellvätskors (Carbopol) radiella strömning mellan parallella plattor. Denna typ av strömningsgeometri används ofta som en idealiserad konfiguration för strömning i bergsprickor. I jämförelse med andra enklare geometrier, finns endast en begränsad forskning utförd för denna geometri både då det gäller analytiska och numeriska beräkningar men framförallt då det gäller experiment. Som ett första steg inför en mer systematisk undersökning av icke-Newtonsk radiella strömning presenteras i detta arbete framtagandet av en fysisk laboratoriemodell där hastighetsprofilerna mellan plattorna för första gången visualiserats med hjälp av ultraljud. De utförda mätningarna med tre olika öppningar mellan plattorna sam tre olika värden på det konstanta flödet, visar på en distinkt plugg som är ett resultat av vätskans flytgräns samt glidning i gränsskiktet mellan vätskan och plattornas fasta begränsningsytor. En jämförelse mellan uppmätta hastighetsprofiler och analytiskt beräknade diskuteras där resultaten överensstämmer relativt väl, med beaktande av de långtgående förenklade antaganden som krävs för beräkningarna.

Fortsatta studier kommer att fokuseras på att förbättra laboratoriemodellen för en mer detaljerad studie av icke-Newtonska vätskors strömning och hur pluggen utvecklas under den radiella inträngningen, vilket fortsättningsvis är av betydelse för design av injektering i bergsprickor.

Preface

The research presented in this licentiate thesis was carried out mostly at the Division of Soil and Rock Mechanics, Department of Civil and Architectural Engineering, at KTH Royal Institute of Technology in Stockholm, Sweden. Most of the experimental work related to the radial flow model was carried out at Incipientus AB, Gothenburg.

The work was supervised by Adj. Professor Ulf Håkansson at Skanska/KTH, Professor Stefan Larsson at KTH and co-supervised by Dr Johan Wiklund at Incipientus AB. Their support, encouragement, and valuable insights towards my work are greatly appreciated. I would like to thank Dr Reinhardt Kotzé and Michal Kotzé at Incipientus for their contributions, especially during my time in Göteborg.

Dr Liangchao Zou from the Resources, Energy and Infrastructure Division at KTH is also acknowledged for his valuable support and for the fruitful discussions which we had over the course of my research studies.

Much thanks goes to my colleagues and friends at the Division of Soil and Rock Mechanics for their engaging questions during our group seminars. The input from my reference group is also gratefully acknowledged.

Last but certainly not least, I am grateful towards my mother Beatrice, and my partner Kristin, for their beloved support, especially during the most demanding times of my work.

Stockholm, June 2019

John Shamu

Funding acknowledgement

The research presented in this thesis was co-funded by the Swedish construction industry's organization for research and development (SBUF) and the Swedish Rock Engineering Research Foundation (BeFo). Their support is gratefully acknowledged.

List of appended papers

Paper I

Shamu, Tafadzwa John, and Ulf Håkansson. "Rheology of Cement Grouts: On the Critical Shear Rate and No-Slip Regime in the Couette Geometry." *Submitted to Cement and Concrete Research*, February 2019.

I carried out the entire experimental work and wrote the paper. Ulf Håkansson supervised the research work and assisted with the comments.

Paper II

Shamu, Tafadzwa John, Liangchao Zou, R Kotzé, Johan Wiklund, and Ulf Håkansson. "Radial Flow Velocity Profiles of a Yield Stress Fluid between Smooth Parallel Disks." *Submitted to Rheologica Acta*, April 2019.

I carried out the entire experimental work and wrote the paper. Liangchao Zou contributed to the data analysis with the analytical solution, and with his comments to the paper. Reinhardt Kotzé and Johan Wiklund provided some ideas to the radial model design, supervised the experimental work in Göteborg and provided their comments to the paper. Ulf Håkansson supervised the entire research endeavor and contributed to the writing of the paper.

Other publications

This article was presented at the BeFo bergmekanikdag 2019 as a direct contribution towards the Licentiate research work; however it is not appended as part of this thesis.

Shamu, John, Liangchao Zou, and Ulf Håkansson. "Cementbaserade Injekteringsmedels Reogram: Instabilt Flöde Och Inverkan På Injektering." In *Bergmekanikdagen*, 19, March 2019.

Contents

1 Introduction

1.1 Background

Cement-based grouting of rock fractures to minimize water inflows into underground constructions e.g. in tunnels is common practice, especially in Scandinavia (Hässler, 1991; Håkansson, 1993; Stille, 2001; Funehag, 2007; Gustafson et al., 2013; Fransson et al., 2016; Nejad Ghafar, 2017; Rahman et al., 2017; Zou et al., 2018; Zou et al., 2019).

The widespread use of cement-based grouts is due to their relatively low cost, combined with the fact that they pose less of a risk as a pollutant especially to underground water resources when compared to other chemical-based grouts. The effectiveness of the grouting process depends on several factors, with the main ones being: rock fracture geometry, grouting design and execution, as well as the penetrability and rheological flow properties of the cement grouts that are used. It has been shown analytically and through experiments, that the rheological properties of cement grouts significantly influence grout propagation during the grouting process, and consequently the final spread and sealing effect that can be achieved in grouted rock fractures (Håkansson, 1993; Gustafson et al., 2013). Thus, carrying out cement grout rheometry with a higher degree of accuracy and understanding the underlying flow phenomena are important issues that still need to be addressed.

To measure these rheological properties, several test methods for the field and laboratory have been developed, with the most common laboratory test being offline rotational rheometry. The resultant flow curve data from rotational tests of cement grouts is often fitted with the Bingham model, which is a simplified model often used to describe the flow behavior of yield stress fluids (YSF). However, this simplification does not take into account phenomena such as flow localization in the form of: (i) shear banding (linked to the critical shear rate of thixotropic suspensions) and (ii) shear localization (due to geometry), that leads to unstable flow. The former type of localization which is linked to the intrinsic physical properties of thixotropic suspensions e.g. cement grouts, laponite and drilling muds, is still an interesting issue, with much discussion in the literature (Pignon et al., 1996; Philippe Coussot et al., 2002; Divoux et al., 2016; Bonn et al., 2017; Rubio-Hernández et al., 2018; Qian & Kawashima, 2018).

However, in the literature there has not been much research work detailing the unstable flow branch as seen in the flow curves of cement grouts, particularly at low shear rates (< 10 1/s) (Rubio-Hernández et al., 2018; Qian & Kawashima,

2018). In order to get a detailed understanding of such unstable flow behavior, a study consisting of systematic rotational rheometric tests was carried out on typical cement grouts, as presented in this thesis.

Furthermore, in relation to cement grout flow and the influence of rheological properties, is the study of radial flow of a simple YSF between smooth parallel plates, which was also part of the current research work. Radial flow in which a fluid penetrates the center of two disks and flows out radially is of interest to applications such as rock grouting design. This fundamental flow configuration ideally simulates cement grout propagation from a central injection borehole from where the grouts spread radially outward into surrounding fractures. The plug flow region of the velocity profile of a YSF is directly related to the yield stress property of the fluid, since the plug region is an unsheared region, wherein the shear rates are close to zero and shear stresses are below the yield stress. Only a limited amount of works have presented analytical and numerical solutions describing the expected velocity profiles for YSFs in this flow geometry. Thus, an experimental study as a first step towards verifying existing theory, together with the measurement of the shape of the plug flow region across the radial length also formed a major part this work.

1.2 Project and thesis aim

The overall aim of the licentiate research project is to carry out two experimental studies with the main objectives of understanding cement grout rheological properties and experimentally modelling two-dimensional (2D) radial flow within the context of grouting applications, whilst taking into account the most recent developments in rheological studies. In short the aims are as follows:

(i) To understand the existence of the critical shear rate, unstable flow and wall slip for typical cement grouts (at water-to-cement ratios of 0.6-0.8).

(ii) The unstable flow, wall slip, critical shear rate and related phenomena are to be studied whilst varying: three different concentric cylinder geometries and three measurement intervals.

(iii) In the end, the goal is to carry out an assessment of how the fitted Bingham properties are affected.

Additionally, the aims from the radial flow experiments are:

(iv) To design an experimental radial flow model that is to be used for studying radial flow velocity profiles of a model YSF (Carbopol).

(v) The model is to be equipped with instrumentation, consisting of an acoustically characterized ultrasound sensor, which is an integral part of the (Ultrasound Velocity Profiling) UVP system to be used for velocimetry.

(vi) Develop a preparation procedure for Carbopol fluid that can be used for velocimetry whilst maintaining the desired simple YSF behavior (non-thixotropic).

(vii) Lastly, the objective is to measure for the first time, time-averaged velocity profiles within the radial flow geometry. The ultimate goal in subsequent studies is to use the developed model to study in detail the nature of the plug flow region.

1.3 Outline of thesis

The thesis will start by presenting a literature review that is based on the two appended scientific papers (Paper I and II). The first part of the review will focus on cement grout rheological measurements and the following sections will review literature related to the radial flow experiments. The review also describes previous work that has been carried out to highlight the relevance and significance of the current studies.

The methods and experimental procedures that were used to address the objectives outlined under Section 1.2 will then be described in detail (Chapter 3). Chapter 4 will then focus on the results of the current observations, followed by a summary of the appended papers in Chapter 5. Chapter 6 will conclude by giving a discussion, conclusions and suggestions for future work. All references cited are then listed under Chapter 7.

1.4 Limitations

The limitations of the current work are mainly based on the measurement techniques that were used for each specific study. For example, the first study on offline rheometry of cement grouts could have been improved by combining the rotational tests with a visualization technique to track the particle concentrations, especially for the vane in cup geometry where sedimentation most likely occurred. Also, the origins of the mechanisms behind the observed phenomena (wall slip, shear banding) were not discussed in detail; however, references to articles discussing these matters were included. For the second study on velocimetry

measurements, the spatial and lateral resolution could have been improved by using a higher frequency transducer. Some of these limitations are then taken into account as suggestions for future work.

2 Theory and literature review

Overall, the theory and literature review is divided into two sections. Section 2.1 and its corresponding subsections focus on scientific literature related to the measurements of cement grout rheology, the Bingham properties, associated flow phenomena and their application to grouting. Section 2.2, mainly describes the relevance of the radial flow configuration to grouting applications by describing some of previous work that has been carried out thus far.

2.1 Cement grout rheological measurements

2.1.1 Significance of cement grout rheological properties

Extensive research over the years has shown that the rheological properties of cement grouts are critical to the success of grouting operations (Håkansson, 1993; Håkansson et al., 1992; Gustafson et al., 2013; Gustafson al., 2013; Rahman et al., 2017; Funehag & Thörn, 2018; Zou et al., 2019). The current state of research related to cement grout flow properties has now reached an advanced level, at which new technologies for quality monitoring e.g. ultrasound based measurements are now being tested and developed for the improvement of grouting applications (Rahman et al., 2015; Rahman et al., 2017). However, from a fundamental standpoint, there is still a lot of work to be done in understanding the underlying phenomena that complicate the flow of cement grouts. Furthermore, the need to improve the quality of cement-based grouting has increased in recent years due to stricter stipulations on water ingress into e.g. tunnels (Gustafson et al., 2013). By understanding these phenomena grout flow can be characterized more effectively, for improved design and execution.

Without considering significant contributions from hydration, fresh cement grouts are known to be complex thixotropic yield stress fluids (YSF) (Roussel, 2005a; Banfill, 2006). To describe this rheological behavior, constitutive models, e.g. the Herschel-Bulkley (HB) and Bingham model are used. The model equations are described below as follows:

$$\tau = \tau_0^B + \mu_B \dot{\gamma} \quad (1)$$

$$\tau = \tau_0 + k\dot{\gamma}^n \quad (2)$$

where for the Bingham model (Equation 1) the yield stress is τ_0^B, the Bingham (plastic) viscosity is μ_B and for the Herschel-Bulkley model τ_0 is the yield stress, k is the consistency coefficient and n is the flow index; for all models τ is the

shear stress and $\dot{\gamma}$ the shear rate (Håkansson, 1993; Chhabra & Richardson, 2008). Usually, the two-parameter Bingham model is used to describe the flow data of many fluids due to its simplicity, although it has been shown that models such as the HB are better at describing the lower shear rate data of shear thinning fluids such as cement grouts. The fitted Bingham properties are then used in analytical solutions and numerical schemes to estimate the maximum grout spread, I_{max} and the corresponding characteristic time of grout spread, t_0. The maximum spread and characteristic grouting are given as:

$$I_{max} = \Delta p \cdot b/2\tau_0 \, ; \, t_0 = 6\Delta p \mu_B/{\tau_0}^2 \tag{3}$$

where, Δp is the effective grouting pressure (difference between imposed grouting pressure p_g and opposing ground water pressure p_w in the rock); μ_B is the grout viscosity (Bingham), b the fracture aperture and τ_0 the yield stress (Bingham) of the cement grout (El Tani, 2012; Gustafson et al., 2013; El Tani & Stille, 2017; Zou et al., 2018).

2.1.2 Cement grout thixotropy and the critical shear rate

As previously mentioned, the Bingham model is simplistic, and like most constitutive flow equations assumes ideal 'simple' yield stress fluid (YSF) behavior, in which all shear rates are attainable under steady state conditions. The idealized Bingham model describes the yielding of a fluid by a sharp transition; whereas, the actual case for real fluid systems is often a complicated process, which occurs over a characteristic range of stresses (Balmforth et al., 2014). The transition from a 'solid-like' regime or state of rest (i.e. state in which there is a higher resistance to flow due to higher elementary particle interactions) to a 'liquid-like' regime after yielding, involves complex flow phenomena, with transient regimes, e.g. as observed even for a model (simple) YSF such as Carbopol over long periods of time (Divoux et al., 2011; Divoux et al., 2012; Divoux et al., 2016).

For highly thixotropic suspensions e.g. cement grouts, laponite suspensions yielding is further complicated by their intrinsic physical properties, leading to shear bands, combined with slip phenomena (Coussot et al., 2006; Møller et al., 2006; Divoux et al., 2016; Rubio-Hernández et al., 2018). Of particular interest to the current work in this thesis, is the existence of a critical shear rate that is a prominent characteristic of thixotropic suspensions and mostly associated with shear banding. A flow phenomenon such as shear banding complicates the interpretation of flow curve measurements, since the flow behavior within the

shear banding regime is unstable and does not correspond to the steady homogenous flow that is required for rheometry.

Previous experimental studies with rotational rheometry and visualization techniques such as Magnetic Resonance Imaging (MRI) have shown that at low shear rates corresponding to stresses within the vicinity of the yielding stress; there exists a certain range of shear rates below which no-steady, homogenous flow is attainable. This contrasts with simple YSF fluids that continue to flow in steady state, even at very low applied shear stress, as seen from long duration creep experiments (Philippe Coussot et al., 2002; Møller et al., 2006; Bonn et al., 2017). Thus, for thixotropic fluids that continue to go under structural build-up at low constant shear rates, the result is abrupt flow stoppage as soon as the applied shear rate in the sheared fluid falls below the critical shear rate, $\dot{\gamma}_c$.

2.1.3 Difficulties of rotational rheometry of cement grouts

Besides shear banding, the rheology of suspensions involves other complex flow phenomena related to suspensions' physical properties e.g. shear localization, wall slip, and sedimentation, which have been the subject of many experimental studies (Bhatty & Banfill, 1982; Saak et al., 2001; Kalyon, 2005; Ballesta et al., 2008; Divoux et al., 2016). Although some general descriptions on how these processes occur, there is still a lot of research going on to fully understand the origins of these phenomena, since shear geometry and measurement protocol, (i.e. preparation of grouts, flow history, flow curve measurement time) play a key role in the flow of thixotropic fluids.

For example, shear localization due to the rheometer geometry also occurs in YSFs in addition to shear banding. In the case of the concentric cylinder geometry (Couette), the shear stress decreases radially outward by a factor of $1/r^2$ from a maximum at the surface of the inner rotor to a minimum at the outer cylinder wall (r are the different values of radial locations between the inner and outer walls of the rheometer gap). Thus, shear localization in the Couette occurs at a radial position where the local stress falls below the yield stress (Divoux et al., 2016).

Moreover, sedimentation and wall slip have been described in literature as having a significant influence on the flow curve data. Wall slip of thixotropic suspensions has been described extensively in the literature, with some generalizations being made for its origins; nevertheless, this question remains open for complex fluid systems such as cement-based grouts. Through velocimetry, wall slip is often identified by a finite (non-zero) velocity at the fluid-solid wall interface. The presence of wall slip during rheometric measurements results in lowered shear

stresses as observed from the measured flow curves. The slip effect is normally reduced by using roughened geometry walls, and for suspensions such as cement grouts the vane tool is often used (Barnes & Nguyen, 2001).

Despite the reduction of slip by the vane geometry, recent studies with the vane have shown that this geometry is also prone to significant sedimentation, secondary flow and non-cylindrical flow streamlines (Ovarlez et al., 2011). The consequences of sedimentation are increased measured stresses especially in the low shear rate range (~< 10 1/s for cement grouts), and these effects have been shown to increase with increasing flow curve measurement duration. These artefacts should be considered when using the vane geometry (Bhatty & Banfill, 1982; Ovarlez et al., 2011; Ovarlez et al., 2012).

Overall, the complications associated with the rheology of cement based grouts as reviewed in this section were considered as part of this work. Specific details to the test methods used within this study are provided in Section 3.1, whilst making reference to Paper I.

2.2 Velocity profile measurements of a YSF in radial flow

2.2.1 Radial flow: relevance to grouting applications

When grouting design is carried out several assumptions and simplifications are carried out in order to estimate the propagation and spread of grouts in fractures (Hässler, 1991; Håkansson, 1993; Stille, 2015; Zou et al., 2018). As described in Section 2.1, cement grout rheological behavior is often simplified by using constitutive laws e.g. the Bingham model. When combined with the rock fracture geometries the entire flow configurations can then be approximated as one-dimensional (1D) channel flow and two-dimensional (2D) flow e.g. radial flow between parallel disks. An illustration of such simplifications is depicted in Figure 2.1.

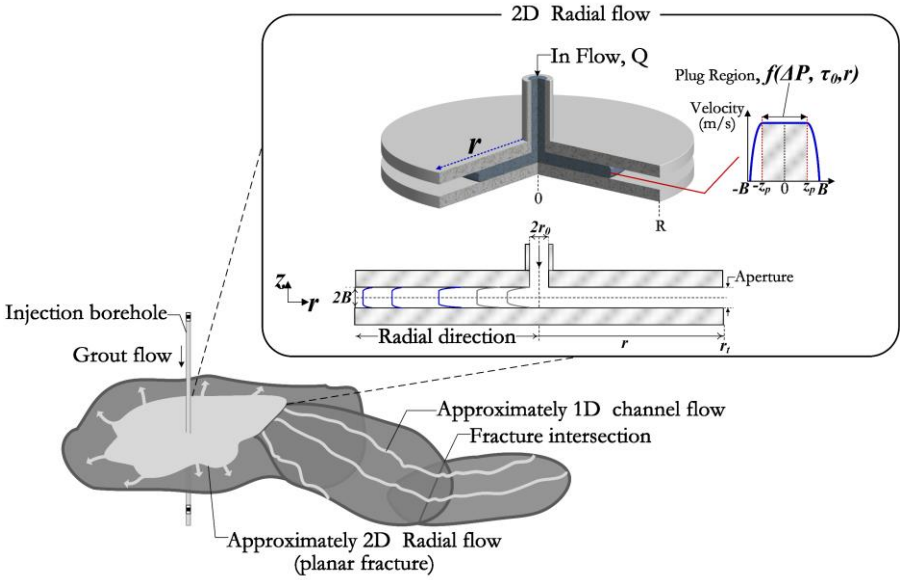

Figure 2.1: Schematic illustrating the idealized 1D channel and 2D radial flow between parallel disks, adapted from (Zou et al., 2018).

A number of analytical solutions describing the flow of Bingham fluids between parallel disks have been presented in the literature (Dai & Byron Bird, 1981; Lipscomb & Denn, 1984; Huang et al., 1987; Gustafson & Stille, 2005; El Tani, 2012; Gustafson et al., 2013; El Tani & Stille, 2017). Usually the underlying assumptions that are used to derive these analytical solutions are that: the aperture is constant throughout the radial length, cement grouts as Bingham fluids are incompressible, the flow is laminar and developed, and that the lubrication approximation (i.e. the aperture dimension is much smaller than the radial length) is valid. Although these analytical models facilitate the estimation of grout penetration, it has to be mentioned that they are largely simplifications especially when the actual geometry of fissures is unknown and the validity of such approaches still needs to be verified for different apertures and fluids (Frigaard et al., 2017).

Within this thesis a constant flow rate analytical solution for yield-power-law (HB) fluids is presented for verification of the measured velocity profiles. The solution is described here as outlined in Paper II and in (Zou et al., n.d.).

Based on the assumption of lubrication approximation, the analytical velocity profiles for incompressible yield-power-law fluids, steady-state, laminar, radial flow between parallel disks can be expressed as

$$v_z^f(z_p < z \leq B) = \frac{n}{n+1}\left(-\frac{1}{k}\frac{\partial P}{\partial r}\right)^{\frac{1}{n}}\left[\left(B - z_p\right)^{\frac{n+1}{n}} - \left(z - z_p\right)^{\frac{n+1}{n}}\right] \quad (4)$$

$$v_z^p(0 \leq z < z_p) = \frac{n}{n+1}\left(-\frac{1}{k}\frac{\partial P}{\partial r}\right)^{\frac{1}{n}}\left(B - z_p\right)^{\frac{n+1}{n}} \quad (5)$$

where v_z^f is the velocity for the yielding flow parts between the edges of plug flow region (z_p) and the walls (B), v_z^p is the velocity for the plug flow region, $\frac{\partial P}{\partial r}$ is the pressure gradient, r and z are the radial and vertical coordinates, k is the consistency coefficient, n is the flow index, and z_p is half of the plug flow region (Figure 2.1), expressed as

$$z_p = \frac{\tau_0(r_t - r_0)}{(P_1 - P_2)} \quad (6)$$

where τ_0 is the yield stress, P_1 and P_2 are the pressure at the inlet r_0 and outlet r_t. The flowrate Q is obtained by integration of the velocity over the aperture, written as,

$$Q = \int_0^B 4\pi r\, v_z\, dz = \frac{4\pi r n}{n+1}\left(-\frac{1}{k}\frac{\partial P}{\partial r}\right)^{\frac{1}{n}} B^{\frac{2n+1}{n}}\left(1 - \frac{z_p}{B}\right)^{\frac{n+1}{n}}\left[1 - \frac{n}{2n+1}\left(1 - \frac{z_p}{B}\right)\right] \quad (7)$$

2.2.2 A review of radial flow experiments of yield stress fluids

For the purposes of validating analytical predictions, experimental studies are carried out to verify the extent to which theoretical assumptions are valid and how they can be further developed based on experimental observations. For instance in the case of 1D YSF flows in, e.g. channels and pipes, several studies and papers have reported analytical solutions, together with experimental investigations and numerical simulations extensively describing these flow configurations (Chhabra & Richardson, 2008). With the use of velocimetry and flow visualization methods such as Particle Image Velocimetry (PIV), Magnetic Resonance Imaging (MRI) and pulsed Ultrasound Velocity Profiling (UVP), experimental studies validating theory have shown in detail, the shape of laminar

flow velocity profiles for different YSFs within these flow configurations (McCarthy et al., 1997; Pfund et al., 2006; Birkhofer, 2007; Powell, 2008; Wiklund et al., 2007; Kotze et al., 2012; Rahman et al., 2017). In contrast, only a limited number of experiments on 2D radial flow of YSFs has been carried out.

Some of the earliest experimental work conducted by e.g. Laurencena & Williams (1974), compared radial flow measurements of the pressure distribution along the radial length, as well as the measured flow rates to analytical predictions, whilst using different power-law fluids, including Carbopol gels, which are also used in our current study. The results from their work showed a good agreement between theoretical predictions and the measurements; however, they strongly suggested that elasticity-induced secondary flows and flow instabilities are highly expected for more concentrated polymer gels as evidenced with tracer injections in their experiments. More recently, the work by Majidi et al. (2010) also presented flow rates and pressure distributions with Xanthan gum as the test fluid. The numerical and measured data satisfactorily agreed with the analytical solutions based on the yield-power-law fluid model. The main discrepancies in their data at high flow rates were explained by the enlargement of the aperture due to pressure build up. Most of the radial flow experiments that have been carried out in relation to grouting have mainly focused on determining the validity of analytical predictions for grout penetration length, whilst using the Bingham model for cement grouts (Funehag & Thörn, 2018; Mohammed, 2015).

Thus, the work presented in this thesis was aimed at (apparently for the first time), measuring radial flow velocity profiles of a model YSF, to further investigate the nature of these profiles and the shape of the plug flow region, within the current framework grouting research.

3 Experimental methods and procedures

The experimental methods related to rheometric tests of cement grouts are first presented under Section 3.1, followed by a description of radial flow model design and test methods in Section 3.2.

3.1 Cement grout rheological measurements

As described in the theory and literature review section, the interpretation of rheological flow curves of fresh cement grouts as measured in the concentric cylinder geometry is complex. This complexity arises mainly due to the intrinsic thixotropic behavior, wall slip and sedimentation amongst other factors. In an effort to reliably measure the flow curves of thixotropic cement grouts it is common to prepare the material in a standardized way i.e. considering mixer type, mixing time and sample loading into the rheometer, before measurement (Fernàndez-Altable & Casanova, 2006; Ovarlez, 2012). However, due to different types of concentric cylinder geometries that can be used, e.g. vanes, grooved cups and grooved rotors to reduce slip, significantly different Bingham properties maybe obtained.

In addition, the measurement interval (time per shear rate or shear stress) allowed for a reasonable steady state condition to be reached at each shear rate or shear stress during the up/down flow curve measurement also influences the overall results (Banfill & Saunders, 1981). The data that is most affected lies in the lower shear rate range (e.g. $\sim< 10\ 1/s$) for grouts; in this range flow effects such as slip, shear banding occur resulting in flow curves that differ from those predicted by simple YSF models such as the HB and Bingham model. Therefore, after establishing a consistent preparation protocol the methods described hereafter were aimed at systematically testing:

(i) the effect of measurement interval t_w on the measured flow curves (Banfill & Saunders, 1981; Shaughnessy & Clark, 1988; Cheng, 2003).

(ii) the effect of concentric cylinder geometrical conditions on the resulting flow curves of typical cement grouts at water to cement (w/c) ratios of 0.6 and 0.8 (Shaughnessy & Clark, 1988; Banfill & Saunders, 1981).

By doing so, the variation of observed flow effects, e.g. decreasing branch of the flow curve due to unstable flow below the critical shear rate coupled to wall slip and sedimentation could be observed. Also, the consequences of these effects on

measured rheological data could then be generalized to a greater extent for grouts studied under different rheometric conditions, since the preparation is standardized.

3.1.1 Preparation procedure of cement grouts

The preparation protocol used to prepare batches for rheological tests during the studies presented in this thesis are based on suggested methods for rheological measurements of thixotropic suspensions and previous research at KTH (Banfill & Saunders, 1981; Philippe Coussot et al., 2002; P. Coussot et al., 2002; Coussot et al., 2006; Ovarlez, 2012; Mashuqur, 2015). The aim when preparing different batches of cement grouts for rheological measurements is to fully disperse the cement powder to obtain a homogenous cement mix, whilst ensuring that factors such as the mixer type, mixing time and sample loading times are noted for the sake of repeatability (Roussel, 2005b; Fernàndez-Altable & Casanova, 2006; Williams et al., 1999).

For the current study, the focus was on studying the behavior of pure grouts without the effect of additives; however, it is pointed out here that the generalized effect of additives such as superplasticizers is a lowered flow curve (i.e. lower yield stress), but still qualitatively resembling the one obtained for a pure grout with the same flow w/c ratio. Cement grouts at w/c were prepared from Cementa Injektering 30 (CEM I 52,5 N - SR 3 LA). A high shear mixer (VMA, Dispermat CV30, and D-51580) was used for dispersing the cement in water for ~4 minutes at ~10 000 rpm (Figure 3.1). This type of mixing resulted in fully dispersed and homogenous cement grout mix that was then used for rheological tests.

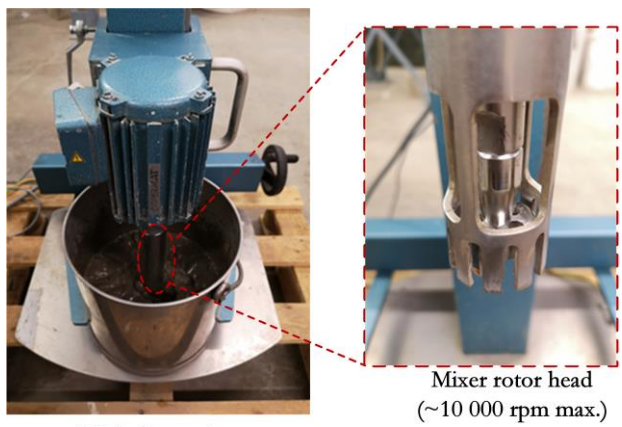

Figure 3.1: High shear cement grout mixer used with rotor head (right)

3.1.2 Preliminary measurements

The selection of measurement intervals t_w to be used in the subsequent systematic study, was based on some of the preliminary measurements carried out in the initial stages of the Licentiate work, plus the previous work at KTH (Mashuqur, 2015).

For the preliminary work, flow ramps (short measurement intervals compared to sweeps) were done by loading a sample of grout into a TA-AR 2000ex rheometer at KTH, by first performing a pre-shear and rest procedure to eliminate any sample loading stresses and to establish a common reference state for all grout mixes. The DIN concentric cylinder geometry was used: rotor with a height of 42 mm and 28 mm in diameter, and a smooth cup with a 30 mm diameter. Successive controlled shear rate (CSR) flow ramps were then carried out and plotted on the same flow curve axis so that the evolution of flow curves due to thixotropy, and possibly early hydration effects could be visualized. Each up/down cycle lasted about ~5 minutes, i.e. 240 s of measurement plus the pre-shearing and rest procedure); therefore the first up/down cycle is labelled as '0 mins' and the last after ~5 minute intervals is '30 mins' (see Figure 3.2).

These preliminary flow curve measurements showed the evolution of cement grouts with time. Also, Figure 3.2b and Figure 3.2c highlight a characteristic drop with some curvature in the flow curve data particularly at low shear rates (i.e. below 10 1/s), signaling wall slip and unstable flows. Moreover, the flow curves in Figure 3.1 also illustrate the importance of plotting flow curves in linear logarithmic format to reveal the signature flow behavior characteristic to thixotropic suspensions such as grouts, that might otherwise be disregarded when the linear format is used.

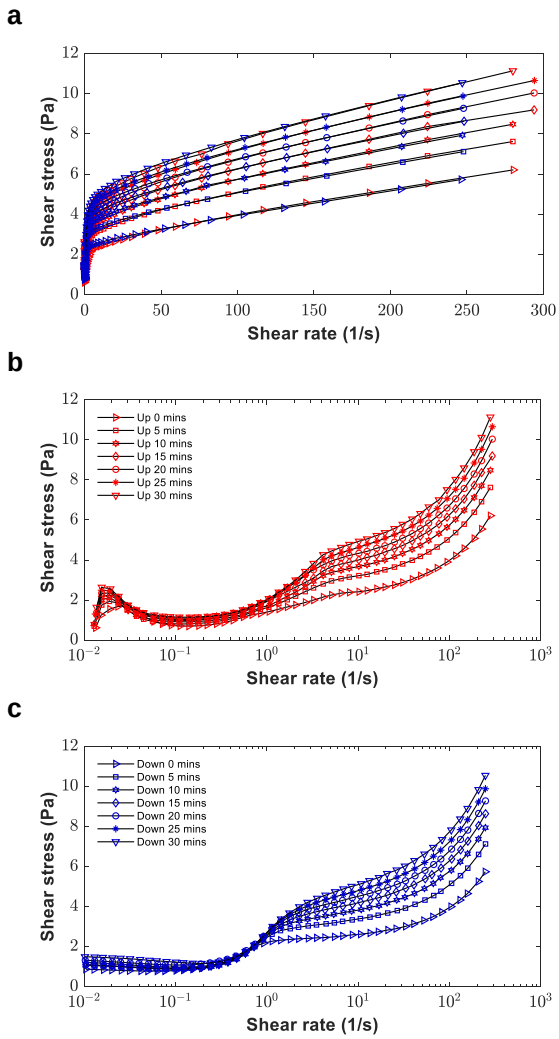

Figure 3.2: Cement grout flow curves (w/c = 0.8) obtained with smooth rotor and cup geometry and with a 240 s cycle time (a) linear plot; linear-logarithmic plots (b) Up curves (c) Down curves highlighting slip and unstable flow effects at (< ~10 1/s)

These initial measurements showed that even when short measurement intervals (t_w=~3 s) and one geometry (smooth cup and rotor) are used, cement grout flow curves can be quite complex to interpret. Thus, a more systematic study was then carried out as presented in Paper I, involving 3 different Couette geometries and 3 different measurement intervals.

3.1.3 Flow curve measurement procedure

To investigate the extent to which the final Bingham properties from the flow curves are affected by Couette measurement geometry and measurement interval t_w a standard measurement procedure was developed. The preparation of cement grouts as described in Section 3.1.1 was done for all grouts in the systematic study.

For the 3 different test geometries and 3 measurement intervals, a total of 18 tests were carried out; with 9 tests for grouts with a w/c ratio of 0.6 and 9 with a w/c ratio of 0.8. The measurement intervals were selected with the shortest time being t_w= 4 s, which was close to that used in the preliminary measurements (Section 3.1.2). The other two measurement intervals t_w= 24 s and t_w= 40 s were estimated from step shear rate tests carried out for 100 s at (0.01 and 20) 1/s to ascertain some reasonable steady state time, which was determined to be close to ~60 s. The dimensions of the 3 Couette geometries used are as shown in Figure 3.3.

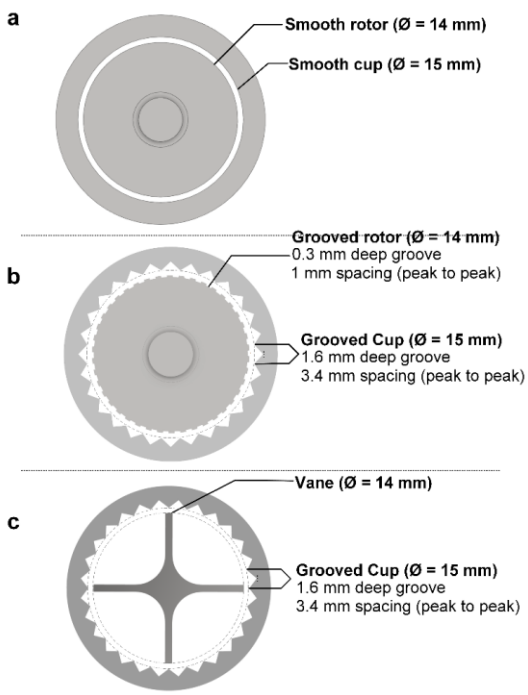

Figure 3.3: Schematics (top cross-section) for the Couette geometries used in the systematic flow curve measurements; (top) smooth cup and rotor, (middle) grooved cup and grooved rotor; (bottom) Vane and grooved cup.

For the 18 flow curves measured a pre-shear of 20 s at 300 1/s, followed by a rest of 30 s was performed. The flow curve measurement was carried out by applying increasing and decreasing flow sweeps in controlled shear rate (CSR) mode. For each flow sweep the shear rate range was between 0.001 to 300 1/s, with 10 points per decade. However, only the flow curves from decreasing shear rates (down curves) were used for the Bingham fitting analysis (see Section 4.1), since the data obtained from down curves is more representative of the grouting condition i.e. starting from higher shear rates (near borehole) down to lower ones. Also, the down curve data is more repeatable within ~10%, compared to the up curves. Additionally, creep measurements were carried out as a further investigative step for flows at low shear rates, where unstable flows due to the critical shear rate are expected. The results of the measurements are summarized in Section 4.1, with reference to the appended Paper I.

3.2 Radial flow experiments

Firstly, a description of the radial flow model design is presented under Section 3.2.1. Secondly, the Ultrasound Velocity Profiling (UVP) method and acoustic tests, to define the critical Doppler angle and sound velocity that are required for velocimetry are presented. Lastly, the preparation of the model YSF Carbopol is then presented together with the rheological test.

3.2.1 Radial model design

The initial design of the physical radial model was based on earlier models presented in the literature (Savage, 1964; Laurencena & Williams, 1974). The aim was to have a radial flow area that was clear of intrusive objects e.g. fasteners, in order to clearly study the underlying radial flow of Carbopol. The entire setup including an image of the actual model used is shown in Figure 3.4.

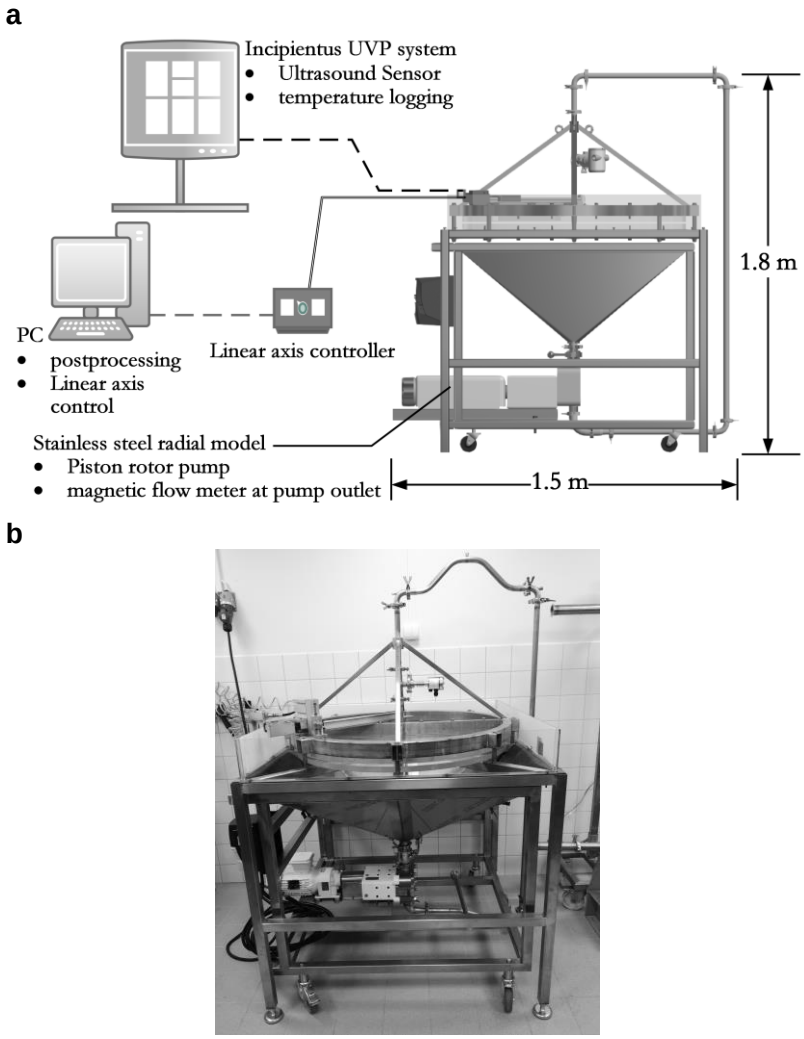

Figure 3.4: (a) A schematic of the radial flow system (b) An image of the physical model

The system components included a magnetic flow meter (Discomag DMI 6531, Endress + Hausser) at the pump outlet and a PT100 temperature transducer. A piston rotor pump was used to pump the fluid at set flow rates controlled from a variable speed drive (VSD). The fluid then circulated from the bottom of the tank into the radial flow area where measurement was carried out. A motorized

linear axis (Isel LEZ 1) with a repeatability of ±0.2 mm was then used to move the ultrasound sensor (US) used for velocimetry, to different radial locations. Schematics and images of the linear axis-slot setup and the radial model are shown in Figure 3.5.

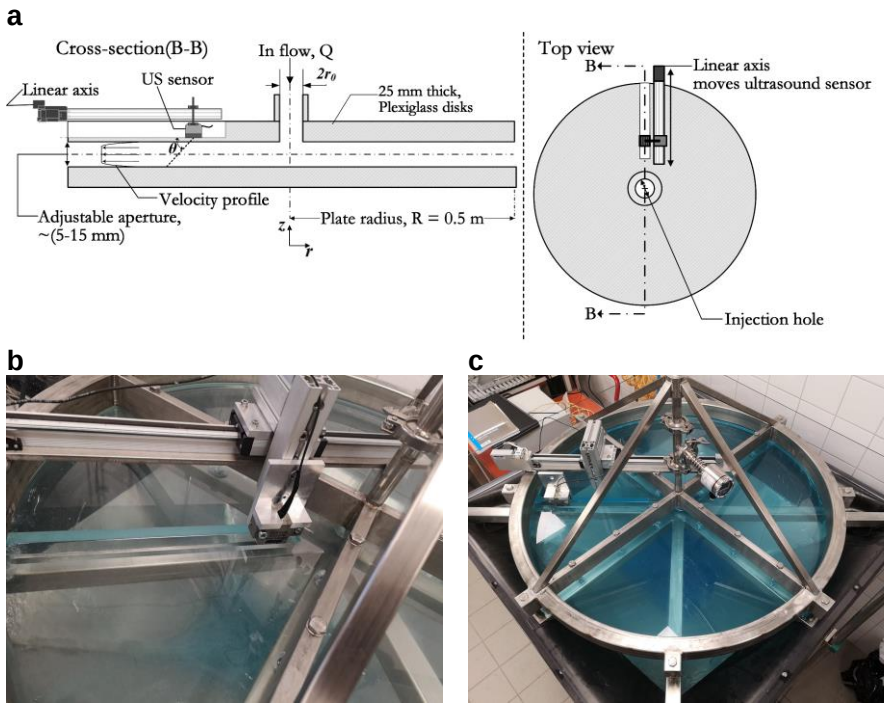

Figure 3.5: (a) schematic of the linear axis setup (b) image showing ultrasound sensor in slot (c) top view image of spoke frame and radial model

The slot shown in Figure 3.5b was machined on the top disk to allow sufficient propagation of the ultrasound beam, without significant attenuation. After machining the wall thickness in the slot was 5 mm. The desired gap (aperture) was achieve by a metallic spacer system around the periphery of the disks. The top spoke frame was used as a support for the top disk, aimed at maintaining the set aperture even during high flow and pressure conditions. The uplift expected during flow conditions was also simulated in the design stage by using a Computer Aided Design (CAD) model developed within Autodesk Inventor® simulation package. From this test, the thickness of the frame members to be used were adjusted such that only negligible uplift (~0.25% displacement in vertical direction) was noted; thus, all tests were considered to be conducted under constant aperture conditions.

3.2.2 Ultrasound Velocity Profiling (UVP) and Acoustic tests

The UVP method used to measure velocity profiles, is a velocimetry method that has been used to acquire velocity profiles in a wide range of complex fluids (Satomura, 1957; Takeda, 1991; Dogan et al., 2005; Pfund et al., 2006; Wiklund et al., 2007; Birkhofer, 2011; Kotze et al., 2012; Takeda, 2012; Rahman et al., 2017). The method relies on the detection of frequency shifts between successive reflected pulses when preprogrammed ultrasound pulses are transmitted into the medium under study. Depending on the flow configuration pulses received from different depths are processed using signal processing algorithms, transforming the measured doppler frequencies (frequency shifts) into velocities that constitute the velocity profile (Barber et al., 1985; Jensen, 1996; Ricci & Meacci, 2018).

The individual velocities v_i at each point of the flow geometry where the velocimetry is carried out are calculated as,

$$v_i = cf_{d_i}/2f_0 cos\theta \tag{8}$$

where f_0 is the central ultrasound transmission frequency, c is the velocity of sound, f_{d_i} the Doppler shift frequency for particles flowing at a certain distance position (gate) and θ is the Doppler angle.

Several studies have shown that the accuracy of velocity estimation depends on the correct determination of the sound velocity in the fluid under study as well as the Doppler angle θ. The error contribution from incorrect angle values is quite significant, therefore, in this work the measurement of this angle was carried out in detail using a needle hydrophone setup as shown in Figure 3.6. For the acoustic tests a plexiglass sheet having the same properties as the wall of the machined slot (Figure 3.5) was attached to the ultrasound sensor measurement surface with an oil-based couplant. The coupled sensor setup was placed in a glass characterization tank with deionized water at ~19 °C. The ultrasound beam from the ultrasound sensor was measured by the needle hydrophone, after propagating through the plexiglass sheet. A rectangular scanning grid (1 mm spatial resolution) across the sensors mid-plane was covered by moving the hydrophone with the linear axis. The scanning method used is described in detail by Shamu et al., (2016); see also Paper II. The output from the acoustic characterization test is an acoustic color map from which the beam angle is determined. For the current study the Doppler angle was ~70.23°.

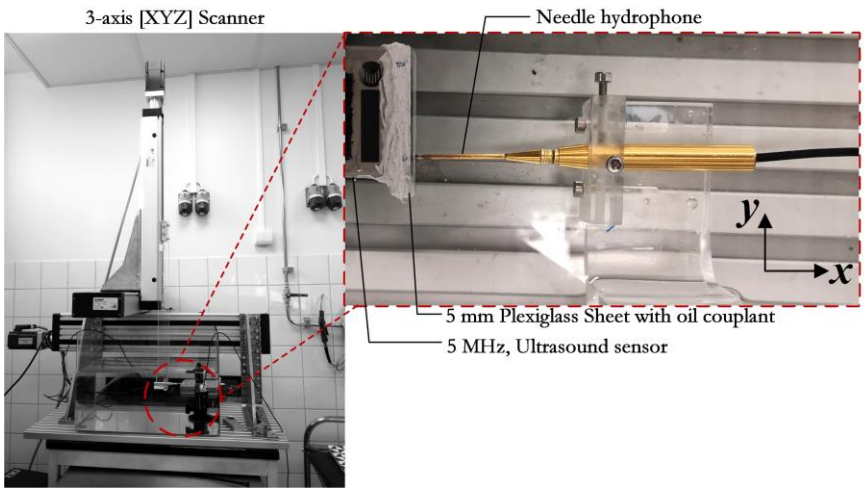

Figure 3.6: Acoustic characterization test setup showing the 3-axis scanner and the needle hydrophone test setup

The sound velocity was measured using a small stainless steel cell setup (diameter of ~31 mm). A Carbopol sample at ~19 °C was placed in the cell and then 12 pulses were transmitted into the sample. By using the Time of Flight (TOF) method, the traversing time was calculated and consequently the sound speed in Carbopol 0.1%wt; an average of ~1500 m/s.

UVP system: Once the correct Doppler angle and velocity of sound were determined, they were then used as input parameters to the UVP software of the Incipientus Flow Visualizer (IFV) system that was used for velocimetry within this study. The IFV has been developed over several years of extensive research for use in in-line rheological measurements of complex industrial fluids (Wiklund et al., 2007; Birkhofer, 2011; Berta et al., 2016; Rahman et al., 2017). The latest developments with the system have been on the ultrasound electronics and non-invasive sensors capable of measuring through industrial steel pipes (Shamu et al., 2016; Ricci et al., 2017; Rahman et al., 2017).

3.2.3 Carbopol gels: preparation and rheology

Carbopol gels prepared from Carbopol 980 (Lubrizol®, Belgium) were used in this study. The Carbomer powder (crosslinked polymer of acrylic acid) is supplied as a white powder which is then dispersed in distilled water, with the appropriate weighting to achieve the desired rheological properties. For the current study Carbopol powder was dispersed at 0.1% wt. of distilled water using a Silverson

AX5 high shear mixer at ~1000 rpm for ~25 minutes (mixer shown in Figure 3.7). The dispersion was left to rest to expel air bubbles and allow complete hydration, before adding reflector particles needed for velocimetry, and a blue colorant. The final step in the preparation procedure was neutralizing the dispersion with dilute sodium hydroxide (18% wt. NaOH) to a final pH of ~6.5-7.5. The neutralization was done with a lower rpm mixer (135 rpm max.), since previous experimenters have shown that high shear mixing during the neutralization phase leads to polydisperse gels that exhibit significant rheological hysteresis (Dinkgreve et al., 2017; Dinkgreve et al., 2018; Di Giuseppe et al., 2015).

After the preparation and also after radial flow measurements in the flow loop the rheology of the Carbopol was measured using a vane (15 mm diameter, 38 mm height) in cup (30 mm diameter) geometry, and at 20 °C. The flow sweep was from 0.001 to 80 1/s with 10 points per decade in CSR mode allowing ~30 s per measurement point. Figure 3.8 shows the flow curve measurement. The measurement shows that the Carbopol exhibits simple YSF behavior that is well described by the HB model, with little to no observable rheological hysteresis in the flow curve.

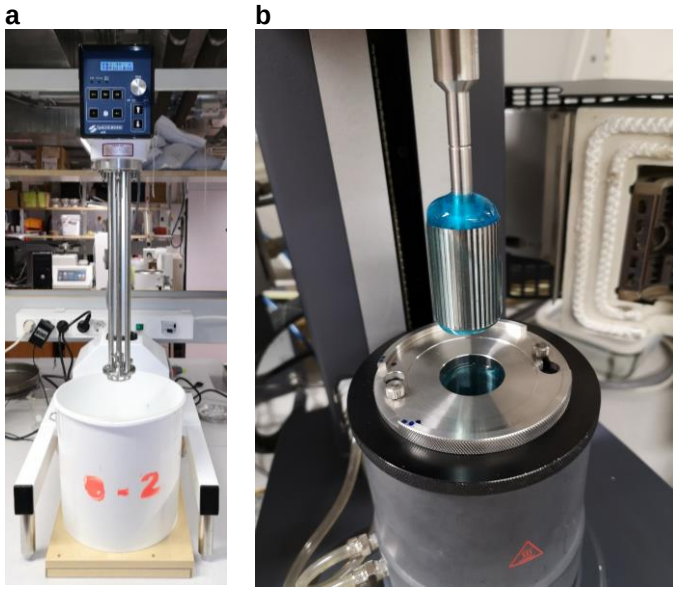

Figure 3.7: (a) High shear mixer (Silverson AX5) for dispersing Carbopol in distilled water (b) Image of a Carbopol gel with additional colorant and acoustic reflector particles.

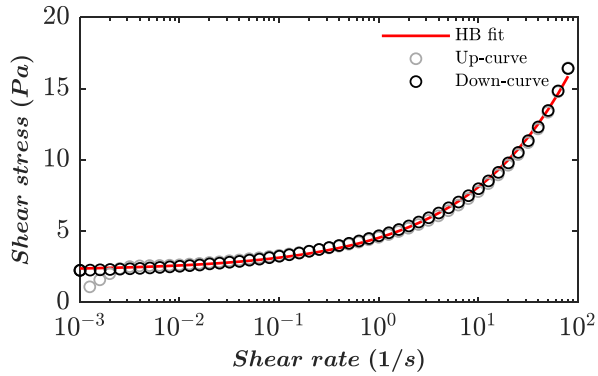

Figure 3.8: Flow curve measurement of Carbopol-980 gel at 0.1% w/w. Herschel Bulkley parameters determined as: τ_0 = 2.24 Pa, k = 2.28 Pa.s^n and n = 0.4.

3.2.4 Radial tests measurement procedure

The test procedure for acquiring radial flow velocity profiles ensures that the fluid measured is homogenous by first circulating the Carbopol fluid in the flow loop (Figure 3.3) for about 2 minutes at a high flow rate of ~58 l/min (similar to pre-shearing in a rheometer). Velocity profile measurements were then carried out by moving the ultrasound sensor to 17 different radial locations i.e. within the slot at radial lengths of 116 mm to 416 mm from the disk' center.

The factors that were varied were: three volumetric flow rates (Q1 = ~28 l/min, Q1 = ~40 l/min Q1 = ~58 l/min) and 3 apertures (5, 10, 15 mm). The fluid temperatures were recorded as ~18.5-20°C. Volume flow rate comparisons between the magnetic flow meter readings and the flow rates determined from the measured velocity profiles were carried out for all measurement conditions. Reasonable agreement was achieved between the two methods of flow rate measurement. However, the major differences were in measurements within the 5 mm aperture. This discrepancy is most probably due to slight increases in the disk aperture due to higher pressure buildup when a small aperture is used. In general the wall position in velocimetry measurements is not well defined for smaller apertures due to the sample volume overlapping the fluid-plexiglass wall interface, which also could have contributed to the uncertainty (Wiklund et al., 2007). This wall issue can however be improved by reducing the number of cycles in an ultrasound pulse and increasing the ultrasound sensor central frequency. A detailed list of ultrasound parameters and test parameters used in this study are listed in Paper II.

Plug region detection: A custom algorithm to detect the plug-flow region in a velocity profile was also developed as part of the radial flow analysis.

The algorithm was based on the CUSUM calculation described by (Grigg et al., 2003), and was implemented with the Matlab® environment. The algorithm (as described in appended Paper II) is as follows:

(i) The velocity profile is normalized ($V_z/V_z max$) and aperture distance (z/B)); and to this normalized profile fit a smoothing spline that minimizes the local fluctuations within the plug region of the profile. These fluctuations when significant, give rise to 'false' plugs due to local minima.

(ii) The standard deviation σ_V from 60% of the velocity points located in the region $[0 \leq z \leq 0.6(B)]$, is calculated as an approximation to the expected fluctuations within the plug region. The value of 0.6 is also an estimate based on the extent of the observable plug region across the aperture. A target median value $\tilde{x}_V$, is then calculated from 25% of the velocity points i.e. $[0 \leq z \leq 0.25(B)]$, these values are at the central core of the velocity profile and hence give a good approximate of the central plug velocity magnitude.

(iii) Using the CUSUM function from Matlab, with inputs from (i) and (ii), the plug position is then determined at the point z_p at which the velocity profile is 6 standard deviations ($6\sigma_V$) less than the target value ($\tilde{x}_V$).

4 Results

Within this chapter the main findings from the flow curve measurements of cement grouts are summarized first under Section 4.1, followed by the results from velocity profiles measured in the radial flow model (Section 4.2)

4.1 Cement grout rheological tests

4.1.1 Flow curves: CSR flow sweeps in Couette geometry

Several flow effects were observed in the measured flow (down) curves, when systematic tests with varying geometry and measurement intervals) were carried out for the two cement grout mixes (w/c = 0.6; 0.8).

Firstly, Figure 4.1 highlights the major difference between flow curves from the completely smooth geometry and vane geometry. The emergence of significant wall slip is seen in the measurements with the smooth rotor-cup geometry, starting at ~10 1/s (Figure 4.1a). With the vane geometry slip was greatly reduced, however the vane data had much higher measured stress values, particularly for longer measurement durations (t_w = 24 s, 40 s) and below the critical shear rate ($\dot{\gamma}_c$), where unstable flow branches are seen (decreasing part of the flow curve) (Figure 4.1b).

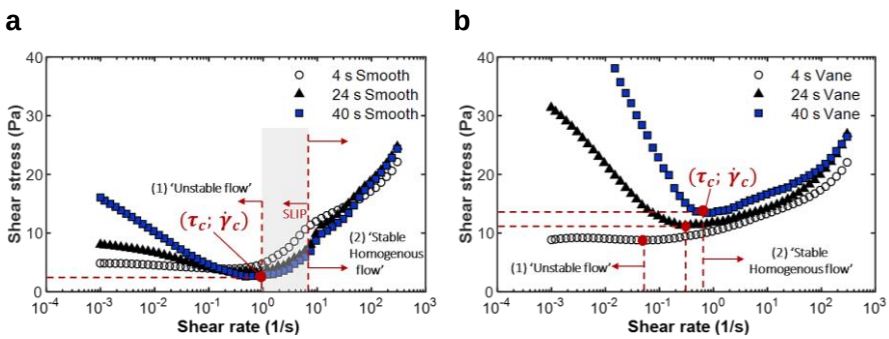

Figure 4.1: Flow curves of grout at (w/c) of 0.6 (a) Smooth cup and smooth rotor (b) Vane and grooved cup

When all the measured flow curves are plotted at once for each grout mix, the offset in the vane data becomes more clear (Figure 4.2).

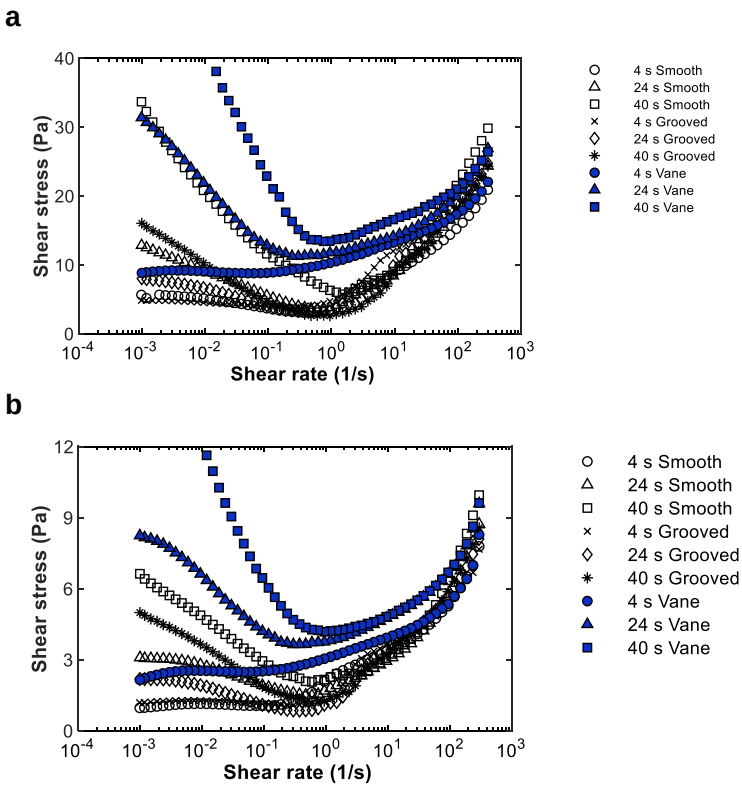

Figure 4.3: Complete set of flow curves for cement grouts at (a) w/c = 0.6 (b) w/c = 0.8, with an unstable flow branch below the critical shear rate. Flow curves in blue symbols show the much higher values measured with the vane, due to thixotropic build-up and sedimentation, particularly at t_w = 24 s and 40 s.

The vane flow curves for both mixes are more agreeable with flow curves from other geometries mainly at the lowest measurement interval of 4 s, particularly for the less concentrated cement grout (w/c = 0.8). This observation supports the idea that thixotropic-build-up, and possibly sedimentation are time dependent processes that occur to a greater extent in the vane geometry. A probable explanation for this observation is that with the vane geometry the material that is trapped between the blades remains stationary and particles are more likely to interact and rebuild in this way. Also, when the particles flocculate to form larger ones, the sedimentation rate increases. Similar observations have been reported in the previous studies on similar materials e.g. cement pastes (Bhatty & Banfill, 1982; Ferron et al., 2013; Ovarlez et al., 2011). Moreover, with the vane and grooved cup and grooved cup setup the presence of secondary flows and non-

cylindrical streamlines that might influence the measurements is possible, as reported by (Ovarlez et al., 2011).

The grooved cup and grooved rotor geometry was expected to reduce slip, however this was not the case. Significant slip was also observed for this geometry although it was slightly less when compared to the completely smooth geometry.

Bingham fitting to assess the impact of the unstable flows below the critical shear rate, wall slip and sedimentation as seen from the measured flow curves, using different geometries and measurement intervals was carried out. Each flow curve was fitted with Bingham fits over two ranges of shear rates:

(i) ($\dot{\gamma}_c$ to $\dot{\gamma}_{max}$), i.e. from the critical shear rate to the maximum measured shear rate. $\dot{\gamma}_c$ was calculated by differentiating the flow curve ($d\tau/d\dot{\gamma}$) and noting the point at which $d\tau/d\dot{\gamma}$ changes sign.

(ii) ($\dot{\gamma}_{NS}$ to $\dot{\gamma}_{max}$), i.e. from the lowest shear rate at which there was no observable slip feature, $\dot{\gamma}_{NS}$. The value of $\dot{\gamma}_{NS}$ was taken at the lowest point of intersection between the Bingham fit ($\dot{\gamma}_c$ to $\dot{\gamma}_{max}$) and the measured flow curve (see e.g. Figure 4.4).

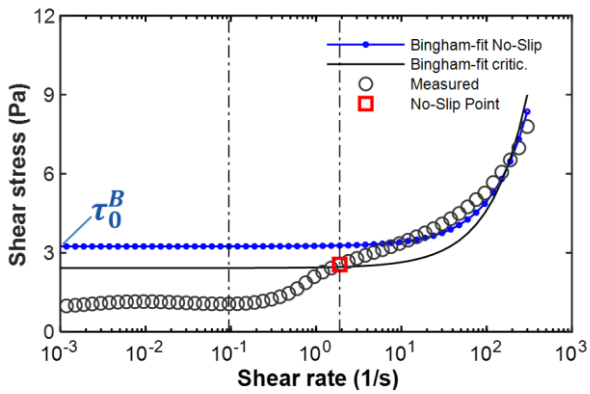

Figure 4.4. Example flow curve of cement grout (w/c = 0.8), measured at t_w= 4 s using a grooved (cup and rotor) geoemtry used to show the two shear rate ranges and Bingham fits. The dashed line at ~0.01 1/s corresponds to $\dot{\gamma}_c$ and the one at 2 1/s is for $\dot{\gamma}_{NS}$

The range of values for the two shear rates $\dot{\gamma}$ and $\dot{\gamma}_{NS}$ is shown in Figure 4.5.

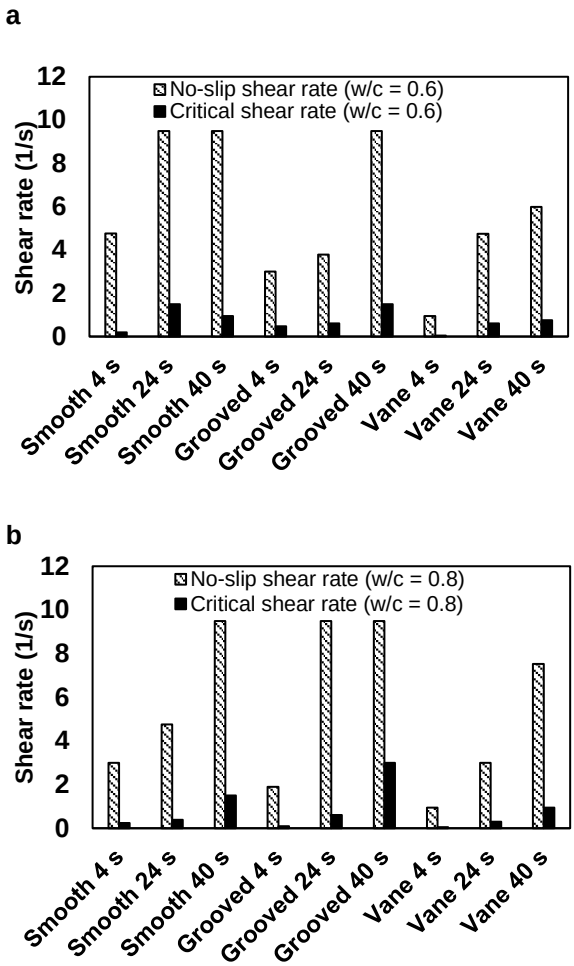

Figure 4.5: Values of the critical and No-slip shear rates for all flow curves, with (a) w/c = 0.6 and (b) w/c = 0.8

In general the results of the Bingham fitting exercise show that slip reduces the Bingham yield stress by as much as ~50% for the completely smooth geometry, when fits in the two shear rate ranges are compared. The vane data showed the least difference (~10%) in Bingham properties determined within the two shear rate ranges; however, Bingham fits to the vane had higher yield stresses particularly for longer measurement intervals. These differences are shown in Figure 4.6.

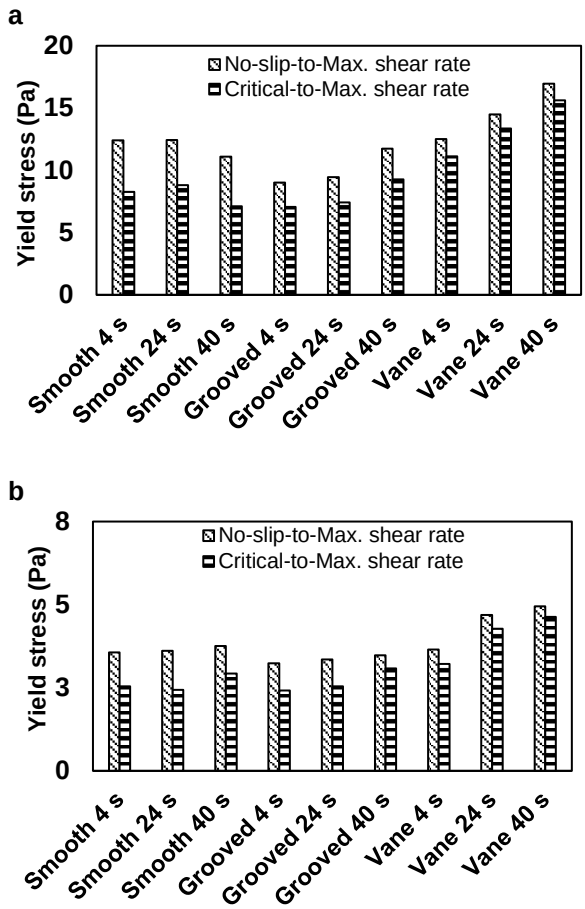

Figure 4.6: Comparison of the Bingham yield stress from the two shear rate ranges (a) w/c = 0.6 and (b) w/c = 0.8

A complete set of critical shear rate values, Bingham Properties and Normalized Root Mean Square Errors (NRMSE) as a measure of goodness of model fitting are tabulated in Paper I. As a final step in the analysis of flow curve measurements, creep tests in Figure 4.7 also confirm the existence of the critical shear rate ranging between ~(0.1 – 1) 1/s (see Paper I).

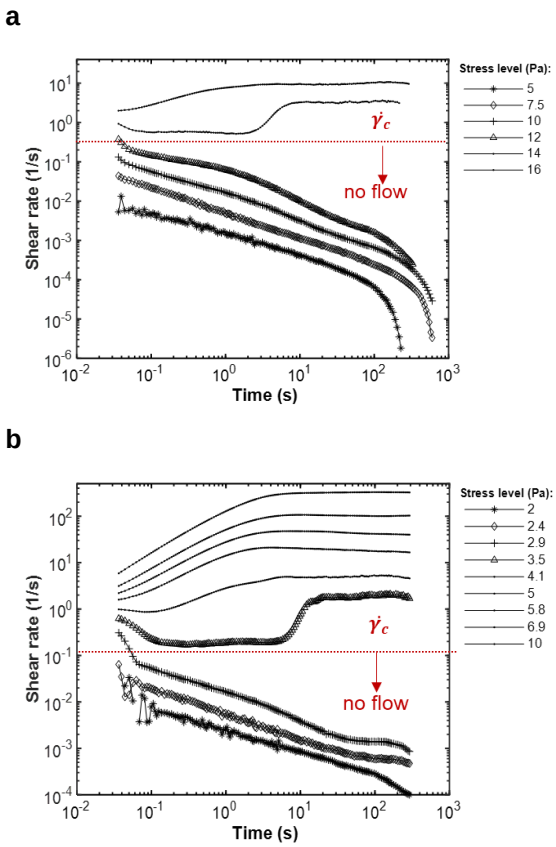

Figure 4.7: Creep tests carried out to confirm unstable flows leading to flow stoppage at stress levels below 3.5 Pa and 14 Pa for grouts at w/c ratios of 0.8 and 0.6 respectively. The critical shear rate is within the range ~(0.1 – 1) 1/s

4.2 Radial flow model results

The velocity profiles measured within the radial flow model are presented in this section. The complete set of velocity profiles consists of 51 profiles per aperture, i.e. 17 different locations, at 3 flow rates per each of the 3 apertures. The velocity profiles are presented for the half-aperture, under the assumption that the velocity profile is axis-symmetric across half the aperture. Also, multiple reflections that are common in velocity profiles determined from UVP measurements distort the far wall data (i.e. opposite to the transducer wall).

4.2.1 Plug flow region and slip effects

An analysis of the velocity profiles carried out by normalizing the velocity profiles, i.e. scaling each velocity profile by its maximum central plug velocity $V_z max$ and the half aperture distance by the half of the aperture length B, gives $V_z/V_z max$ and z_p/B respectively. By plotting contour colormaps (Figure 4.8a,b,c) of the velocity profiles measured over the entire radial length, the rapid decrease in velocity magnitude, plus the distinct plug flow region are visualized. Also, the normalized profiles when overlaid in Figure 4.8d,e,f, show the relative extent of the plug region based on the CUSUM calculation, and the ratio of the slip velocity at the wall compared to the central plug velocity. Here, the contour plots and normalized velocity profiles are presented only for 1 flow rates and 3 apertures (see Paper II).

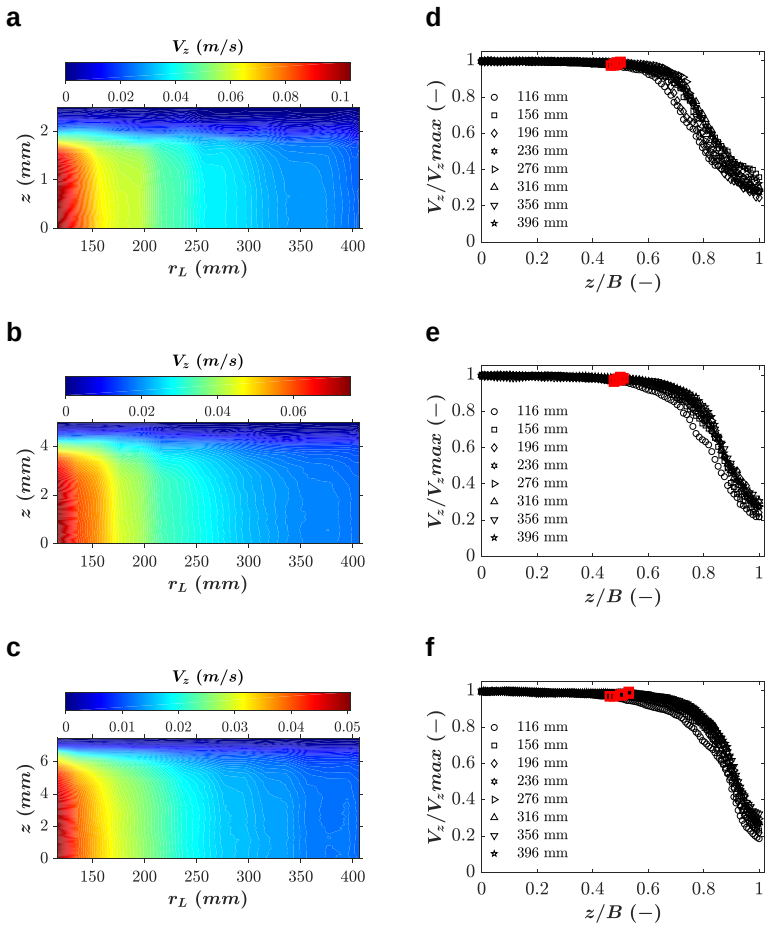

Figure 4.8: Contour colormaps of the velocity profiles at ~40 l/min, for apertures (a) 5 mm (b) 10 mm (b) 15 mm; the corresponding normalized velocity profiles (d) 5 mm (e) 10 mm (f) 15 mm. The red squares are plug region positions based on the CUSUM calculation.

As expected, significant wall slip effects were observed by the presence of finite wall velocities in all the measured velocity profiles. The slip velocity as a ratio of the maximum velocity per velocity profile (V_s/V_zmax) ranged between ~0.2-0.4 (Figure 4.8). Moreover, possibly due to slip, the CUSUM based plug ratios (z_p/B), were much larger ranging from ~0.45 to 0.55, compared to a maximum plug ratio of $z_p/B = 0.21$ predicted for the 15 mm aperture at the lowest flow rate. An elaborate analysis of these plug ratios is presented in Paper II.

4.2.2 Velocity profile comparisons with analytical solution

In Figure 4.9, the analytically predicted velocity profiles are compared to the measured velocity profiles.

For all flow conditions, the magnitudes of the velocity profiles were within the same order of magnitude, and a good agreement was seen for profiles measured in the 5 mm aperture. However, it has to be pointed out that the 5 mm gap there could have been slight aperture increase due to much higher internal pressures, and hence the lowered velocity magnitude. However, this issue needs further investigation as part of the next study. Moreover, in general the analytical solution understated the velocities for the larger apertures 10 mm and 15 mm. It might be the case that the larger entrance effects expected in the 10 mm and 15 mm apertures dominate for most of the radial length. In line with this, the agreement between the measured and predicted profiles is improved at the furthest radial location (396 mm) and at the lowest flow rate ~28 l/min. Lastly, the existence of secondary flows for a YSF like Carbopol is highly probable. Earlier radial flow experiments by Laurencena & Williams (1974) with tracer particles strongly suggested the presence of secondary flow, due to Carbopol gels' elasticity. Nevertheless, these and other related flow effects that could have been present in the radial flow data presented here need to be systematically studied and are out of the scope of the current work in this thesis.

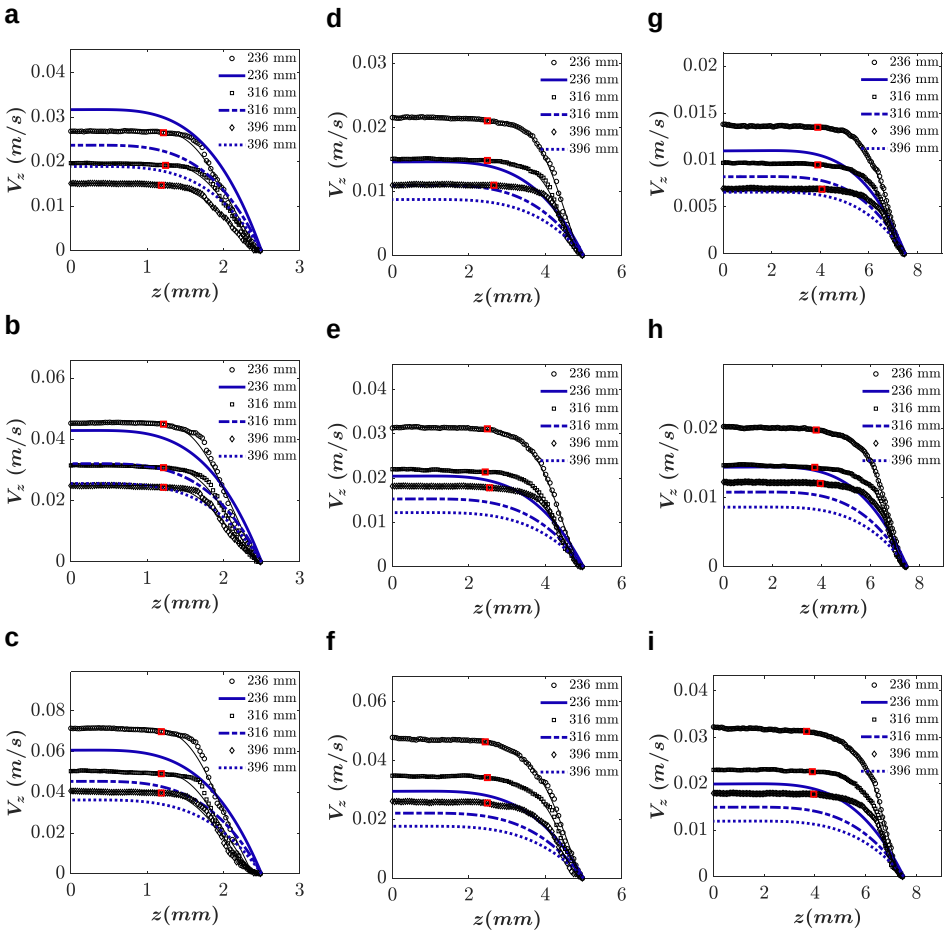

Figure 4.9: Analytically predicted profiles (thick blue lines) plotted together with the measured data (circles), for 5 mm aperture (a) ~28 l/min (b) ~40 l/min (c) ~58 l/min; 10 mm aperture (d) ~28 l/min (e) ~40 l/min (f) ~58 l/min; 15 mm aperture (h) ~28 l/min (i) ~40 l/min (j) ~58 l/min. The thin lines following the measured profiles are the smoothing splines used to estimate plug positions (red squares).

5 Summary of appended papers

5.1 Paper I

Rheology of Cement Grouts: On the Critical Shear Rate and No-Slip Regime in the Couette Geometry

Shamu, Tafadzwa John, and Ulf Håkansson

Submitted to *Cement and Concrete Research*, February 2019.

This paper presents a systematic study that showed the presence of unstable flow behavior in cement grouts below a critical shear rate, coupled to slip effects that tend to complicate the interpretation of rheological flow curves. The factors varied as part of the study were three different Couette geometries (smooth cup and smooth rotor, grooved cup and grooved rotor, vane and grooved cup) and measurement intervals (t_w= 4 s, 24 s, 40 s). The measurement interval and geometries were chosen for the investigation, since they have been noted to be amongst the main factors in the flow curve measurement protocol that lead to significantly different results.

The study was carried out by performing rotational rheometry tests on typical cement grouts (Cementa Injektering 30) used in tunneling projects around Sweden, at water to cement (w/c) ratio of 0.6 and 0.8. A TA AR2000ex rheometer at KTH Byggvetenskap, was used for the rheological tests. The preparation of cement grouts was also described in detail.

The results showed that, for all cement grouts tested, at low shear rates ($\sim< 10$ 1/s), there exists a critical shear rate that lies mainly in the range $\sim(0.1 – 1)$ 1/s, and varies with measurement interval as well as geometry. Due to this critical shear rate an unstable flow branch was revealed and its slope was the greatest for the vane measurements, possibly due to significant structural build-up and sedimentation for the longer duration tests. An assessment of how the unstable flow effects and slip affect the fitted Bingham properties was also presented. Recommended testing procedures were also presented together with some considerations on the possible flow impacts of such flows in actual rock fractures.

5.2 Paper II

Radial Flow Velocity Profiles of a Yield Stress Fluid between Smooth Parallel Disks

Shamu, Tafadzwa John, Liangchao Zou, R Kotzé, Johan Wiklund, and Ulf Håkansson

Submitted to *Rheologica Acta*, April 2019.

This paper presents experimental work carried out to design a radial flow model to study radial flow of a YSF between smooth parallel disks. The aim of the work was to show, for apparently the first time, the nature of velocity profiles measured within the radial flow configuration with UVP. The relevance of the work is that, 2D-radial flow is an idealized flow configuration that is normally used as a simplification during grouting design to estimate radial spread of cement grouts in planar fractures; however, this complex flow configuration still needs to be studied in detail.

The paper describes the entire design process involved in setting up the radial flow model. This included descriptions of how the flow area was achieved (5 mm, 10 mm, 15 mm apertures) through a metallic spacer configuration. In addition, the acoustic characterization of the 5 MHz ultrasound sensor to determine the Doppler angle that is critical for velocimetry is also described. The preparation of Carbopol gels with acoustic reflector particles was detailed in the paper, with emphasis on the use of low shear mixing during the neutralization phase, so as to avoid thixotropic gels. Magnetic flowmeter volumetric flow rates agreed quite well with the velocity profile determined ones, however the velocity profile flow rates were generally much lower for the 5 mm gap. A CUSUM based algorithm to estimate the plug-flow region was presented. The experimentally measured plug ratios were larger than those predicted by the analytical solution possibly due to slip effects. As part of the analysis the analytically predicted velocity profiles were compared to the measured values, and a reasonable agreement was achieved especially for profiles at low flows and furthest from the central injection point. The major discrepancy was that the analytical velocity profiles had lower magnitude, especially for the measurements with larger apertures. This was explained by the fact that the analytical solution which is based on the lubrication assumption, might be more valid for much smaller apertures relative to the radial length, and for the larger apertures, entrance effects could have been greater. Additionally, the presence of secondary flow components was not ruled out as affecting the overall flow dynamics due to the known elasticity inherent in polymeric YSF fluids e.g. Carbopol.

6 Discussion, conclusions and suggestions for future work

6.1 Rheology of cement grouts

6.1.1 Discussion

The work on cement grout rheology presented in this thesis as well as in the appended Paper I, was aimed at studying the unstable flow behavior of thixotropic cement grouts, which has also been shown to exist for other thixotropic suspensions e.g. Laponite, cement pastes. The unstable flow behavior is strongly linked to the critical shear rate ascribed to localization of flow, i.e. shear banding and shear localization in the literature (Olmsted, 2008; Ovarlez et al., 2009; Ovarlez, 2012; Divoux et al., 2016; Bonn et al., 2017).

By conducting tests in the CSR mode of the rheometer, with three different geometries and three measurement intervals (4 s, 24 s, 40 s) an unstable flow branch (decreasing flow curve) was observed at low shear rate in the measured flow curves. The unstable branch had a slope that increased with the measurement interval of the flow sweep. This unstable branch has been described as being linked to strongly localized flow and possibly the coupled effect of wall slip. In general the critical shear rate was estimated to be in the range ~0.1-1 1/s for the cement grouts tested in this work with w/c ratios of 0.6 and 0.8. For the geometries tested, the vane reduced wall slip significantly. However, the main drawback of the vane is probably its susceptibility to secondary flows, as well as increased structural build-up and sedimentation as a result of the stationary material in between the blades, leading to much higher measured stresses throughout the measurement shear rate range when compared to other geometries. The grooved rotor was expected to reduce slip significantly, however this was not the case. Slip mechanisms for thixotropic suspensions are not yet well understood in the literature, however we assume that the geometry wall roughness has to be dimensioned accordingly to the particle sizes in the fluid (Coussot, 2005; Bonn et al., 2017).

An assessment of the Bingham fits in two shear rate ranges for all grouts was then presented to determine the impact of unstable flow and wall slip whilst using different Couette geometries and measurement intervals. Firstly, from this analysis, the range of critical shear rates as seen in the flow curves as well as the creep tests was identified. Secondly, the significantly reduced Bingham yield stress due to wall slip when using the smooth geometry was discussed, whilst noting the differences between fits obtained from the two shear rate ranges. Thirdly, general recommendations to improve rheological characterization of cement grouts

which are normally conducted using the Couette configuration were outlined (see Paper I). Lastly, the impact of the observed flow behavior, (i.e. unstable flow below the critical shear rate, wall slip, thixotropic build-up) in flow of grouts in actual rock fractures were also considered. It might be the case that, in low flow rate conditions that arise at further grouting distances from the injection borehole; the wall shear rate in such flow, might then fall into the range of the critical shear rate, resulting in unstable flow and abrupt flow stoppage. Similarly, another possible scenario is when grouting is momentarily stopped and started again after significant structural build-up in the grout has formed a material structure that is stronger than the initial one.

6.2 Radial flow of YSF between parallel disks

6.2.1 Discussion

2D-radial flow is an important flow configuration, and in grouting it is idealized as an approximation to radial grout spread in planar fractures. Analytical solutions have been presented for the radial flow configuration, however a few works have presented experimental studies to investigate the nature of radial flow velocity profiles, with focus on the plug-flow region that is associated to the yield stress of the fluid (Laurencena & Williams, 1974; Dai & Byron Bird, 1981; Lipscomb & Denn, 1984; Majidi et al., 2010; Mohammed, 2015; El Tani & Stille, 2017; Guo et al., 2017; Funehag & Thörn, 2018).

The study on radial flow presented in this work (Paper II), described the overall design of the radial flow model that was manufactured for measuring 2D radial flow velocity profiles, whilst using Carbopol a simple YSF, as the model fluid. In addition, the ultrasound sensor used for the radial flow experiment was also characterized to improve the accuracy of the measurements. Three apertures and three volumetric flow rates were used. A motorized linear axis was then moved to different radial locations to measure velocity profiles at constant flow conditions (flow rate, aperture).

An analysis of the measured velocity profiles showed that there was significant wall slip, which was expected due to the smooth walled plexiglass disks. The mechanism of slip which was assumed to be prevalent in the Carbopol radial flows, is that in which a thin micron-sized water-based film in the vicinity of the wall surrounds the bulk homogenous YSF. The consequence of the wall slip phenomena is less shear deformation within the bulk of the fluid, and hence the larger 'much flatter' measured plug-flow regions compared to the theoretical ones. The positions of the plug were calculated by using a CUSUM based algorithm that was developed as part of the current study. The plug detection

algorithm proved to be effective since similar profiles were correctly assessed as having the same plug values.

When the theoretical profiles were compared to the analytical solution (Section 2.2), there was relatively good agreement at low flow rates and at the furthest points from the central inlet e.g. at 396 mm, and ~28 l/min. The agreement of the velocity profile magnitudes for the 5 mm apertures was greater; however, it must be noted that there was probably an aperture increase due to higher pressure build-up for the smallest aperture (5 mm). Additionally, the uncertainty in the wall position was higher for the 5 mm velocity profile measurements due to the sample volume overlapping with the wall interface.

6.3 Conclusions

In summary, the entire work that was carried out in this licentiate work was aimed at understanding rheological measurements related to cement-based grouts and in general YSFs, and their application to rock grouting. The main conclusions from this work, are summarized as follows:

- The flow curves of cement grouts show a significant dependency on the measurement interval t_w that is used and the Couette geometry, particularly at low shear rates ($\sim< 10$ 1/s).
- In general, the CSR-based flow curves of cement grouts can be separated into two regions: (i) unstable flow below a critical shear rate $\dot{\gamma}_c$, where flow localization (shear localization and shear banding) is pronounced especially at longer test durations (ii) a steady homogenous shear region for shear rates above $\dot{\gamma}_c$.
- As expected, the flow curves of cement grouts are affected by significant wall slip especially with completely smooth Couette geometry. For other geometries e.g., the grooved rotor and cup, unexpected wall slip was observed. This indicates that for complex suspensions such as cement grouts, wall slip is more complicated and the wall roughness of the rheometer geometry needs to be dimensioned accordingly to the particle size distribution of the cement grains.
- Although the vane be reduces wall slip, it might not be suitable for long duration tests were structural build-up and sedimentation dominate.
- When the flow curves of cement grouts were assessed with Bingham fitting, it was noted that within the homogenous flow region there exists a shear rate range between $\dot{\gamma}_c$ and $\dot{\gamma}_{NS}$, that needs to be excluded from the data used for model fitting (see Table 1 in Paper I). Within this region, data points are affected by wall slip, particularly for the smoother geometries.

As an initial step to studying idealized 2D radial flow of yield stress fluids (YSF), as it applies to grouting applications, the following conclusions were drawn:

- An experimental radial flow model was successfully designed and manufactured for the purpose of measuring, radial velocity profiles of a simple YSF model (Carbopol) flowing between smooth parallel disks.
- The experimental model system components were tested and the ultrasound sensors were acoustically characterized to improve the accuracy of the measurements.
- Time averaged velocity profiles were successfully measured at three different apertures, three different flow rates and radial locations, showing the presence of a distinct plug flow region in all cases.
- As expected, significant wall slip effects were observed by the presence of a finite wall velocity in all profiles, which ranged from ~0.2-0.4 of the maximum profile velocity $V_z max$. After correction of the slip velocity V_s, the measured velocity profiles were lower, but reasonably within the same order of magnitude when compared to the analytically predicted ones. The major discrepancies were explained by: the larger entrance effects in the larger geometries, probable aperture increase in 5 mm gap due to pressure buildup and also the likely presence of secondary flow effects that have been reported in previous studies.
- A CUSUM based algorithm was developed for this work to identify the extent of the plug flow region. The algorithm was efficient and robust enough to identify similar plug regions for similar profiles (see Sections 3.2.4 and Paper II).
- The calculated plug region from the measured velocity profiles were larger than those predicted by the analytical solutions, possibly due to wall slip that reduces the deformation in the shear region of the profile.

On the whole, the studies showed that the rheological properties of YSFs can be measured with a higher degree of accuracy by considering the geometrical contributions (wall condition) and other mechanisms such as wall slip, thixotropy, flow localization, secondary flow and sedimentation complicate that tend to complicate the overall flow dynamics. Some of these flow phenomena e.g. secondary flow were not considered in detail as they were out of the scope of the current work. However, to better describe cement grout spread in rock fractures such complex mechanisms need to be considered as part of future studies.

6.3.1 Suggestions for future work

As part of the conclusions of the current work, some suggestions for future work are also summarized:

- Further work to complement the current work would be a more detailed study of cement thixotropy, to develop more realistic models to describe cement grouts' flow. The developed models can then be implemented in e.g. numerical models, that are used to predict with greater accuracy the expected flow conditions.

- Also, studying the evolution of the rheological properties of cement grouts through the use of oscillatory based measurements would be important as an estimate to the waiting time required between grouting cycles.

- In addition to studying the flow phenomena that affect cement grout flow properties with the use of offline methods, it is also necessary to further investigate and develop in-line rheometric methods e.g. based on the UVP technique (Rahman et al., 2015; Rahman et al., 2017; Ricci et al., 2017). Such techniques are aimed at ensuring quality control of grouts during the grouting process. Furthermore, with such methods, the capability for digital logging and post-analysis of grouting execution is enhanced, possibly leading to improved grouting results.

- For future work, the aim is to further study the nature of the plug-flow region, which remains an interesting fundamental question and especially for grouting design, where the radial flow configuration is often used. To carry out this detailed work, the current setup of the radial flow model could be improved by using higher frequency ultrasound sensors and different pulsar settings for enhanced lateral and axial resolution.

- The CUSUM method for plug detection that was developed as part of the current work, can still be improved, especially its robustness through testing different fluids and by varying the ultrasound measurement settings. In addition, the radial model spoke frame can be further reinforced with radial beams to prevent possible disk uplifts during high pressure flow conditions.

7 References

Ballesta, P., Besseling, R., Isa, L., Petekidis, G. & Poon, W.C.K. 2008. Slip and flow of hard-sphere colloidal glasses. *Physical Review Letters*, 101(25). http://arxiv.org/abs/0807.1437 27 November 2018.

Balmforth, N.J., Frigaard, I.A. & Ovarlez, G. 2014. Yielding to Stress: Recent Developments in Viscoplastic Fluid Mechanics. *Annual Review of Fluid Mechanics*, 46(1): 121–146.

Banfill, P.F.G. 2006. Rheology of fresh cement and concrete. *Rheology reviews*, 2006: 61.

Banfill, P.F.G. & Saunders, D.C. 1981. On the viscometer examination of cement pastes. *Cement and Concrete Research*, 11: 363–370.

Barber, W.D., Eberhard, J.W. & Karr, S.G. 1985. A new time domain technique for velocity measurements using Doppler ultrasound. *Biomedical Engineering, IEEE Transactions on*, (3): 213–229.

Barnes, H.A. & Nguyen, Q.D. 2001. Rotating vane rheometry — a review. *Journal of Non-Newtonian Fluid Mechanics*, 98(1): 1–14.

Berta, M., Wiklund, J., Kotze, R. & Stading, M. 2016. Correlation between in-line measurements of tomato ketchup shear viscosity and extensional viscosity. *Journal of Food Engineering*, 173: 8–14.

Bhatty, J.I. & Banfill, P.F.G. 1982. Sedimentation behaviour in cement pastes subjected to continuous shear in rotational viscometers. *Cement and Concrete Research*, 12(1): 69–78.

Birkhofer, B. 2011. Doppler Ultrasound-Based Rheology. In I. T. Norton, F. Spyropoulos, & P. Cox, eds. *Practical food rheology: an interpretive approach*. Food science and technology. Chichester, West Sussex ; Ames, Iowa: Wiley-Blackwell.

Birkhofer, B.H. 2007. *Ultrasonic In-Line Characterization of Suspensions*. Zurich, Switzerland: Laboratory of Food Process Engineering Institute of Food Science and Nutrition Swiss Federal Institute of Technology (ETH) Zurich ETH Zentrum, LFO 8092 Zurich Switzerland.

Bonn, D., Denn, M.M., Berthier, L., Divoux, T. & Manneville, S. 2017. Yield Stress Materials in Soft Condensed Matter. *Reviews of Modern Physics*, 89(3). http://arxiv.org/abs/1502.05281 17 August 2018.

Cheng, D.C.-H. 2003. Characterisation of thixotropy revisited. *Rheologica Acta*, 42(4): 372–382.

Chhabra, R. & Richardson, J. 2008. *Non-Newtonian Flow and Applied Rheology*. 2nd ed. Oxford, UK: Butterworth-Heinemann.

Coussot, P. 2005. Experimental Procedures and Problems in Paste Viscometry. In *Rheometry of Pastes, Suspensions, and Granular Materials*. Hoboken, NJ, USA: John Wiley & Sons, Inc.: 81–152. http://doi.wiley.com/10.1002/0471720577.ch3 29 October 2018.

Coussot, Philippe, Nguyen, Q.D., Huynh, H.T. & Bonn, D. 2002. Avalanche Behavior in Yield Stress Fluids. *Physical Review Letters*, 88(17). https://link.aps.org/doi/10.1103/PhysRevLett.88.175501 2 July 2017.

Coussot, P., Nguyen, Q.D., Huynh, H.T. & Bonn, D. 2002. Viscosity bifurcation in thixotropic, yielding fluids. *Journal of Rheology*, 46(3): 573–589.

Coussot, P., Tabuteau, H., Chateau, X., Tocquer, L. & Ovarlez, G. 2006. Aging and solid or liquid behavior in pastes. *Journal of Rheology*, 50(6): 975–994.

Dai, G. & Byron Bird, R. 1981. Radial flow of a Bingham fluid between two fixed circular disks. *Journal of Non-Newtonian Fluid Mechanics*, 8(3–4): 349–355.

Di Giuseppe, E., Corbi, F., Funiciello, F., Massmeyer, A., Santimano, T.N., Rosenau, M. & Davaille, A. 2015. Characterization of Carbopol® hydrogel rheology for experimental tectonics and geodynamics. *Tectonophysics*, 642: 29–45.

Dinkgreve, M., Denn, M.M. & Bonn, D. 2017. "Everything flows?": elastic effects on startup flows of yield-stress fluids. *Rheologica Acta*, 56(3): 189–194.

Dinkgreve, M., Fazilati, M., Denn, M.M. & Bonn, D. 2018. Carbopol: From a simple to a thixotropic yield stress fluid. *Journal of Rheology*, 62(3): 773–780.

Divoux, T., Barentin, C. & Manneville, S. 2011. Stress overshoot in a simple yield stress fluid: An extensive study combining rheology and velocimetry. *Soft Matter*, 7(19): 9335.

Divoux, T., Fardin, M.A., Manneville, S. & Lerouge, S. 2016. Shear Banding of Complex Fluids. *Annual Review of Fluid Mechanics*, 48(1): 81–103.

Divoux, T., Tamarii, D., Barentin, C., Teitel, S. & Manneville, S. 2012. Yielding dynamics of a Herschel–Bulkley fluid: a critical-like fluidization behaviour. *Soft Matter*, 8(15): 4151.

Dogan, N., McCarthy, M.J. & Powell, R.L. 2005. Measurement of polymer melt rheology using ultrasonics-based in-line rheometry. *Measurement Science and Technology*, 16(8): 1684–1690.

El Tani, M. 2012. Grouting Rock Fractures with Cement Grout. *Rock Mechanics and Rock Engineering*, 45(4): 547–561.

El Tani, M. & Stille, H. 2017. Grout Spread and Injection Period of Silica Solution and Cement Mix in Rock Fractures. *Rock Mechanics and Rock Engineering*, 50(9): 2365–2380.

Fernàndez-Altable, V. & Casanova, I. 2006. Influence of mixing sequence and superplasticiser dosage on the rheological response of cement pastes at different temperatures. *Cement and Concrete Research*, 36(7): 1222–1230.

Ferron, R.D., Shah, S., Fuente, E. & Negro, C. 2013. Aggregation and breakage kinetics of fresh cement paste. *Cement and Concrete Research*, 50: 1–10.

Fransson, Å., Funehag, J. & Thörn, J. 2016. Swedish grouting design: hydraulic testing and grout selection. *Proceedings of the Institution of Civil Engineers - Ground Improvement*, 169(4): 275–285.

Frigaard, I.A., Paso, K.G. & de Souza Mendes, P.R. 2017. Bingham's model in the oil and gas industry. *Rheologica Acta*, 56(3): 259–282.

Funehag, J. 2007. *Grouting of Fractured Rock with Silica Sol*. Göteborg, Sweden: Chalmers University of Technology.

Funehag, J. & Thörn, J. 2018. Radial penetration of cementitious grout – Laboratory verification of grout spread in a fracture model. *Tunnelling and Underground Space Technology*, 72: 228–232.

Grigg, O.A., Farewell, V.T. & Spiegelhalter, D.J. 2003. Use of risk-adjusted CUSUM and RSPRTcharts for monitoring in medical contexts. *Statistical Methods in Medical Research*, 12(2): 147–170.

Guo, J., Asce, M., Shan, H., Xie, Z., Li, C., Xu, H., Zhang, J. & Professor, A. 2017. Exact Solution to Navier-Stokes Equation for Developed Radial Flow between Parallel Disks. *J. Eng. Mech.*: 10.

Gustafson, G., Claesson, J. & Fransson, Å. 2013. Steering Parameters for Rock Grouting. *Journal of Applied Mathematics*, 2013.

Gustafson, G. & Stille, H. 2005. Stop criteria for cement grouting. *Felsbau*, 23(3): 62–68.

Håkansson, U. 1993. *Rheology of fresh cement-based grouts*. Stockholm: Royal Institute of Technology.

Håkansson, U., Hässler, L. & Stille, H. 1992. Rheological properties of microfine cement grouts. *Tunnelling and Underground Space Technology*, 7(4): 453–458.

Hässler, L. 1991. *Grouting of Rock - Simulation and Classification*. PhD. Stockholm: Royal Institure of Technology (KTH).

Huang, D.C., Liu, B.C. & Jiang, T.Q. 1987. An analytical solution of radial flow of a bingham fluid between two fixed circular disks. *Journal of Non-Newtonian Fluid Mechanics*, 26(1): 143–148.

Jensen, J.A. 1996. *Estimation Of Blood Velocities Using Ultrasound: A Signal Processing Approach*. Cambridge University Press.

Kalyon, D.M. 2005. Apparent slip and viscoplasticity of concentrated suspensions. *Journal of Rheology*, 49(3): 621–640.

Kotze, R., Wiklund, J. & Haldenwang, R. 2012. Optimization of the UVP+ PD rheometric method for flow behavior monitoring of industrial fluid suspensions. *Applied Rheology*, 22: 42760–1.

Laurencena, B.R. & Williams, M.C. 1974. Radial Flow of Non-Newtonian Fluids Between Parallel Plates. *Transactions of the Society of Rheology*, 18(3): 331–355.

Lipscomb, G.G. & Denn, M.M. 1984. Flow of bingham fluids in complex geometries. *Journal of Non-Newtonian Fluid Mechanics*, 14: 337–346.

Majidi, R., Miska, S.Z., Ahmed, R., Yu, M. & Thompson, L.G. 2010. Radial flow of yield-power-law fluids: Numerical analysis, experimental study and the application for drilling fluid losses in fractured formations. *Journal of Petroleum Science and Engineering*, 70(3–4): 334–343.

Mashuqur, R. 2015. *Rheology of cement grout - Ultrasound based in-line measurement technique and grouting design parameters*. http://www.diva-portal.org/smash/record.jsf?pid=diva2:571272.

McCarthy, K.L., Kerr, W.L., Kauten, R.J. & Walton, J.H. 1997. Velocity Profiles Of Fluid/Particulate Mixtures In Pipe Flow Using MRI. *Journal of Food Process Engineering*, 20(2): 165–177.

Mohammed, M.H. 2015. Study of cement-grout penetration into fractures under static and oscillatory conditions. *Tunnelling and Underground Space Technology*: 11.

Møller, P.C.F., Mewis, J. & Bonn, D. 2006. Yield stress and thixotropy: on the difficulty of measuring yield stresses in practice. *Soft Matter*, 2(4): 274.

Nejad Ghafar, A. 2017. *An Experimental Study to Measure Grout Penetrability, Improve the Grout Spread, and Evaluate the Real Time Grouting Control Theory*. Stockholm: KTH Royal Institute of Technology.

Olmsted, P.D. 2008. Perspectives on shear banding in complex fluids. *Rheologica Acta*, 47(3): 283–300.

Ovarlez, G. 2012. Introduction to the rheometry of complex suspensions. In *Understanding the Rheology of Concrete*. Elsevier: 23–62. http://linkinghub.elsevier.com/retrieve/pii/B9780857090287500029 29 October 2018.

Ovarlez, G., Bertrand, F., Coussot, P. & Chateau, X. 2012. Shear-induced sedimentation in yield stress fluids. *Journal of Non-Newtonian Fluid Mechanics*, 177–178: 19–28.

Ovarlez, G., Mahaut, F., Bertrand, F. & Chateau, X. 2011. Flows and heterogeneities with a vane tool: Magnetic resonance imaging measurements. *Journal of Rheology*, 55(2): 197–223.

Ovarlez, G., Rodts, S., Chateau, X. & Coussot, P. 2009. Phenomenology and physical origin of shear localization and shear banding in complex fluids. *Rheologica Acta*, 48(8): 831–844.

Pfund, D.M., Greenwood, M.S., Bamberger, J.A. & Pappas, R.A. 2006. Inline ultrasonic rheometry by pulsed Doppler. *Ultrasonics*, 44: e477–e482.

Pignon, F., Magnin, A. & Piau, J. 1996. Thixotropic colloidal suspensions and flow curves with minimum: Identification of flow regimes and rheometric consequences. *Journal of Rheology*, 40(4): 573–587.

Powell, R.L. 2008. Experimental techniques for multiphase flows. *Physics of Fluids*, 20(4): 040605.

Qian, Y. & Kawashima, S. 2018. Distinguishing dynamic and static yield stress of fresh cement mortars through thixotropy. *Cement and Concrete Composites*, 86: 288–296.

Rahman, M., Håkansson, U. & Wiklund, J. 2015. In-line rheological measurements of cement grouts: Effects of water/cement ratio and hydration. *Tunnelling and Underground Space Technology*, 45: 34–42.

Rahman, M., Wiklund, J., Kotzé, R. & Håkansson, U. 2017. Yield stress of cement grouts. *Tunnelling and Underground Space Technology*, 61: 50–60.

Ricci, S. & Meacci, V. 2018. Data-Adaptive Coherent Demodulator for High Dynamics Pulse-Wave Ultrasound Applications. *Electronics*, 7(12): 434.

Ricci, S., Meacci, V., Birkhofer, B. & Wiklund, J. 2017. FPGA-Based System for In-Line Measurement of Velocity Profiles of Fluids in Industrial Pipe Flow. *IEEE Transactions on Industrial Electronics*, 64(5): 3997–4005.

Roussel, N. 2005a. Steady and transient flow behaviour of fresh cement pastes. *Cement and Concrete Research*, 35(9): 1656–1664.

Roussel, N. 2005b. Steady and transient flow behaviour of fresh cement pastes. *Cement and Concrete Research*, 35(9): 1656–1664.

Rubio-Hernández, F.J., Páez-Flor, N.M. & Velázquez-Navarro, J.F. 2018. Why monotonous and non-monotonous steady-flow curves can be obtained with the same non-Newtonian fluid? A single explanation. *Rheologica Acta*, 57(5): 389–396.

Saak, A.W., Jennings, H.M. & Shah, S.P. 2001. The influence of wall slip on yield stress and viscoelastic measurements of cement paste. *Cement and Concrete Research*, 31.

Satomura, S. 1957. Ultrasonic Doppler Method for the Inspection of Cardiac Functions. *The Journal of the Acoustical Society of America*, 29(11): 1181–1185.

Savage, S.B. 1964. Laminar Radial Flow Between Parallel Plates. *Journal of Applied Mechanics*, 31(4): 594.

Shamu, T.J., Kotze, R. & Wiklund, J. 2016. Characterization of Acoustic Beam Propagation Through High-Grade Stainless Steel Pipes for Improved Pulsed Ultrasound Velocimetry Measurements in Complex Industrial Fluids. *IEEE Sensors Journal*, 16(14): 5636–5647.

Shaughnessy, R. & Clark, P.E. 1988. The rheological behavior of fresh cement pastes. *Cement and Concrete Research*, 18(3): 327–341.

Stille, H. 2001. Grouting-Research Work and Practical Application. In *4th Nordic Rock Grouting Symposium*. Stockholm.

Stille, H. 2015. *Rock grouting - Theories and Applications*. Stockholm: Vulkanmedia.

Takeda, Y. 1991. Development of an ultrasound velocity profile monitor. *Nuclear Engineering and Design*, 126: 277–284.

Takeda, Y. 2012. *Ultrasonic Doppler velocity profiler for fluid flow*. Tokyo, Japan: Springer. http://link.springer.com/content/pdf/10.1007/978-4-431-54026-7.pdf 29 July 2014.

Wiklund, J., Shahram, I. & Stading, M. 2007. Methodology for in-line rheology by ultrasound Doppler velocity profiling and pressure difference techniques. *Chemical Engineering Science*, 62(16): 4277–4293.

Williams, D.A., Saak, A.W. & Jennings, H.M. 1999. The influence of mixing on the rheology of fresh cement paste. *Cement and Concrete Research*, 29(9): 1491–1496.

Zou, L., Håkansson, U. & Cvetkovic, V. 2019. Cement grout propagation in two-dimensional fracture networks: Impact of structure and hydraulic variability. *International Journal of Rock Mechanics and Mining Sciences*, 115: 1–10.

Zou, L., Håkansson, U. & Cvetkovic, V. Radial propagation of yield-power-law fluids into water-saturated homogeneous fractures.

Zou, L., Håkansson, U. & Cvetkovic, V. 2018. Two-phase cement grout propagation in homogeneous water-saturated rock fractures. *International Journal of Rock Mechanics and Mining Sciences*, 106: 243–249.